Université de Montréal

# Étude de l'inflammation induite lors d'une hémorragie sous-arachnoïdienne

Par Ahmed Najjar

Département de pharmacologie et physiologie

Faculté de médecine

Mémoire présenté
en vue de l'obtention du grade de Maîtrise
ès Sciences (M.Sc.) en
Physiologie moléculaire, cellulaire et intégrative

Mai 2019

Université de Montréal

Faculté de médecine

Ce mémoire intitulé:

# Étude de l'inflammation induite lors d'une hémorragie sous-arachnoïdienne

Présenté par:

Ahmed Najjar

A été évalué par un jury composé de personnes suivantes :

Président-rapporteur : Docteur Réjean Couture

Directeur de recherche : Docteur Jean-François Cailhier

Membre du jury : Docteur Jean-Gilles Guimond

# Résumé

L'Hémorragie Sous-Arachnoïdienne (HSA) est une maladie dévastatrice. L'activation de l'inflammation a déjà été documentée lors d'une HSA. Plus d'information sur cette "neuro-inflammation" est nécessaire afin de comprendre les mécanismes cellulaires et moléculaires induits par une HSA et surtout afin de comprendre comment sa modulation pourrait changer l'évolution des patients. Nous proposons l'hypothèse que l'HSA induit une inflammation et que celle-ci est associée à des lésions des cellules cérébrales responsables des déficits neurologiques des patients. Dans la partie expérimentale, nous avons utilisé le modèle d'injection de sang dans l'espace préchiasmatique pour induire l'HSA afin d'étudier les dommages neuronaux et la charge inflammatoire chez la souris à l'aide de marqueurs immunofluorescents (NeuN, Fluoro-Jade, F4/80), TUNEL et le MPO. Pour la partie clinique, nous avons étudié le caractère de la leucocytose systémique dans deux groupes de patients avec HSA traités chirurgicalement ou par voie endovasculaire. Nous avons montré que notre modèle HSA induit des dommages neuronaux et de l'apoptose chez les souris à 5 et 7 jours qui pourraient être dus à l'inflammation par une activation de microglie/macrophages et/ou de neutrophiles. Du côté humain, l'analyse statistique démontre une leucocytose post HSA qui augmente suite à la chirurgie sans lien avec le devenir clinique. En conclusion, l'inflammation dans le modèle murin pourrait être associée à des lésions neuronales dues à la présence de cellules inflammatoires. La leucocytose systémique est plus importante en chirurgie et pourrait être un acteur important dans le pronostic de l'HSA.

**Mots-clés**: Hémorragie sous-arachnoïdienne (HSA), inflammation, leucocytose

# Abstract

Subarachnoid hemorrhage (SAH) is a devastating disease. Recently, neuroinflammation has been proposed as a key determinant of patient outcomes. However, more information is needed concerning cellular and molecular mechanisms induced by SAH and how this could affect patients' outcomes. We propose the hypothesis that SAH induces inflammation and that this inflammation is associated with brain cell damage and possible worse patient outcomes. For the experimental component of this study, a blood injection model in the prechiasmatic cistern was used to induce SAH and study the degree of neuronal cell death or damage and the inflammatory burden in mice using immunofluorescence staining (NeuN, Fluoro-jade, F4/80), TUNEL and MPO. The clinical component studied the degree of systemic leukocytosis in two standard acute treatment groups after SAH—surgical clipping versus endovascular embolization—to evaluate if leukocytosis affects outcomes between the two groups.

The study showed that there is evidence of neuronal damage and apoptosis in SAH mice at days 5 and 7. This could be due to inflammation by microglia/macrophages and/or neutrophils. The clinical statistical analysis demonstrated that leukocytosis was present initially after SAH, which peaked after the surgical intervention, but did not affect long-term clinical outcomes.

In conclusion, evidence of inflammation in the mouse model was confirmed by neuronal damage and the presence of inflammatory cell activation. Also, in patients, systemic leukocytosis is more important after surgery and could be an important player in the prognosis of SAH, but other inflammatory and clinical parameters should be considered.

**Keywords**: Subarachnoid hemorrhage (SAH), inflammation, leukocytosis

# Content

**RÉSUMÉ** **II**

**ABSTRACT** **III**

**LIST OF TABLES** **VI**

**LIST OF FIGURES** **VII**

**LIST OF ABBREVIATIONS** **VIII**

**ACKNOWLEDGMENTS** **XI**

**1.INTRODUCTION** **1**

1.1 IMMUNE PRIVILEGE OF THE CNS 1

1.2 INNATE IMMUNITY AND THE CNS 2

*1.2.1 Microglia* *4*

1.3 ADAPTIVE IMMUNITY AND THE CNS 8

1.4 IMMUNE RESPONSES IN STROKE AND BRAIN HEMORRHAGE 10

1.5 SUBARACHNOID HEMORRHAGE 11

*1.5.1 Brain anatomy* *11*

*Circle of Willis* *12*

*1.5.2 Epidemiology* *13*

*1.5.3 Pathophysiology* *13*

*1.5.4 Morbidity and mortality* *16*

1.6 INFLAMMATION AND SUBARACHNOID HEMORRHAGE 16

1.7 IMPORTANCE OF MFG-E8 19

1.8 CLINICAL IMPLICATIONS AND ADVANCES IN SAH RESEARCH 20

**2. HYPOTHESES, AIMS AND OBJECTIVES** **23**

2.1 HYPOTHESES, AIMS AND OBJECTIVES 23

**3. EXPERIMENTAL LABORATORY METHODS** **24**

3.1 MICE 24

*3.2 SAH and sham surgeries* *24*

3.3 BRAIN SLIDES PREPARATION 25

3.4 QUANTIFICATION OF NEURONAL DAMAGE AND INFLAMMATION 26

*3.4.1 Hematoxylin and eosin (H&E) staining* *27*

*3.4.2 Immunofluorescence staining (IF)* *27*

*Fluoro-jade staining and neuronal degeneration* *28*
*TUNEL assay and apoptosis* *29*
*MPO staining* *29*

**4. EXPERIMENTAL ANIMAL MODEL RESULTS** **31**

**5.CLINICAL STUDY** **37**

5.1 CLINICAL METHODS 37
STATISTICAL ANALYSIS 39

**6. RESULTS OF THE CLINICAL STUDY** **41**

6.1 DEMOGRAPHIC DATA 41
6.2 PERI-PROCEDURAL PARAMETERS 41
6.3 WBC COUNTS 43
*6.3.1 WBC changes and mRS* *46*
*Evaluation of leukocyte ratios in association with outcomes* *52*

**7. DISCUSSION AND CONCLUSIONS** **53**

7.1 DISCUSSION 53
7.2 CONCLUSION AND PERSPECTIVES 57

**BIBLIOGRAPHY** **58**

# List of Tables

**Table 1 Functions of microglia** ..... **7**

**Table 2 Comparison between M1 and M2** ..... **7**

**Table 3 Specific SAH induced systemic inflammatory responses** ..... **18**

**Table 4 Delayed Cerebral Ischemia and Inflammation** ..... **19**

**Table 5 Mice used to obtain slides. Total of 59 mice including donors and recipients used to conduct staining testing and experiments** ..... **25**

**Table 6 Number of mice used for each staining** ..... **26**

**Table 7 World Federation of Neurosurgery Scale** ..... **38**

**Table 8 Fisher Grade** ..... **38**

**Table 9 Modified Rankin Score** ..... **40**

**Table 10 Demographic variables. SD, standard deviation; CI, confidence interval; F, Female; M, Male; N, Number of patients** ..... **41**

**Table 11 Peri-procedural clinical and laboratory parameters. SD, standard deviation; CI, confidence interval; N, Number of patients** ..... **42**

**Table 12 Mean (±SD) WBC counts at different times peri procedure** ..... **44**

**Table 13 mRS values for surgery and endovascular groups** ..... **47**

**Table 14 Change in WBC count from baseline day 5 and mRS** ..... **49**

**Table 15 Change in maximum WBC count from baseline day 5 and mRS** ..... **51**

# List of figures

**Figure 1 What is an aneurysm? ..... 12**

**Figure 2 NeuN staining. ..... 28**

**Figure 3 Blood in SAH sections. ..... 31**

**Figure 4 Trends for More Degenerated Neurons in SAH ..... 32**

**Figure 5 SAH induces a little more apoptosis. ..... 33**

**Figure 6 F4/80 staining Day 5. ..... 34**

**Figure 7 F4/80 staining Day 7. ..... 35**

**Figure 8 MPO staining. ..... 36**

**Figure 9 WBC differential percentages from days 1 to 5 in the surgery group. ..... 45**

**Figure 10 WBC differential percentages from days 1 to 5 in the endovascular group. ..... 46**

**Figure 11 mRS and WBC day 5 post-intervention. ..... 48**

**Figure 12 Mean maximum change in WBC and mRS. ..... 50**

# List of abbreviations

| | |
|---|---|
| APC | Antigen Presenting Cell |
| BBB | Blood Brain Barrier |
| CBF | Cerebral Blood Flow |
| CD | Cluster of Differentiation |
| CNS | Central Nervous System |
| CSF | Cerebrospinal Fluid |
| CT | Computed Tomography |
| DAPI | 4',6-diamidino-2-phenylindole |
| DCI | Delayed Cerebral Ischemia |
| EBI | Early Brain Injury |
| ICP | Intracranial Pressure |
| IL | Interleukin |
| INFγ | Interferon gamma |
| KO | Knock-Out |
| MAP | Mean Arterial Pressure |
| MAPK | Mitogen-Activated Protein Kinase |
| MFG-E8 | Milk Fat Globule-Epidermal Growth Factor- 8 |
| MHC | Major Histocompatibility Complex |
| MMP | Matrix Metalloproteinase |
| MPO | Myeloperoxidase |
| mRS | Modified Rankin Scale |
| MS | Multiple Sclerosis |

| | |
|---|---|
| NVU | Neurovascular Unit |
| ROS | Reactive Oxygen Species |
| SAH | Subarachnoid Hemorrhage |
| TLR | Toll-Like Receptor |
| TUNEL | Terminal deoxynucleotidyl transferase dUTP Nick End Labeling |
| WBC | White Blood Cell |
| WT | Wild-Type |

*I dedicate this "Memoire" to my wife, Renad who is continuous support during hard times. Also, this has never been possible without the reason for my presence, my parents. I wish this opens or will be part of long-lasting research work at the CRCHUM*

# Acknowledgments

*Without the support of Dr. Michel W Bojanowski, Dr. Jean-François Cailhier, my mentors, I could never have been involved as a part of such an incredible project.*

*Also, I would like to thank Patrick Laplante for his support and help in doing laboratory experiments and providing guidance.*

*Many thanks to Dr.Réjean Couture, director of the graduate program, for the administrative support and guidance.*

# 1.Introduction

## 1.1 Immune Privilege of the CNS

The central nervous system (CNS) is “immune-privileged”, This means that it is capable of protecting itself from the surrounding environment to limit damage and maintain the functions it provides to the body. This immune privilege was originally and partially defined by Billingham and Boswell as the relative tolerance to grafts and the inability of systemic immune cells to invade the CNS because the blood-brain barrier (BBB) acts as an obstacle for hydrophilic molecules at the capillary level. However, leukocytes leave the bloodstream at the post-capillary venule level, thus immune privilege does not prevent leukocytes from infiltrating the CNS (Billingham and Boswell, 1953). Brain antigens cannot elicit but can succumb to an immune response (Medawar, 1948). The cells of the immune system, that reach the brain through the choroid plexus, continuously interact with the CNS, communicating to resident cells what is happening elsewhere.

What makes the CNS unique is the combined presence of the BBB, a special lymphatic system, and highly specialized cells. The BBB comprises brain capillaries that form barriers to certain hydrophilic molecules. The capillaries have special morphological characteristics such as endothelial cells that lack fenestrations at tight junctions. Whether these are parenchymal or meningeal vessels is not known (Dyrna et al., 2013). Another important component of the BBB is the neurovascular unit, which consists of structural barriers beyond the endothelium, including pericytes, astrocyte endfeet, vascular and parenchymal basement membranes, and the glia limitans (Muldoon et al., 2013). It is possible to identify other physical barriers at different anatomical sites within the CNS (e.g., epithelial cells of the choroid plexus, the blood-cerebrospinal fluid barrier). Leukocytes invade parenchyma through two differently regulated steps. First, they pass the vascular wall and the basement membrane. They are not yet in the

parenchyma. There still is the perivascular space separated from the neuropil by a basement membrane, astrocyte, and microglia endfeet building up the glia limitans. The next important step is the cleavage of the basement membrane-endfeet connection by metalloproteinases 2 and 9 (Agrawal et al., 2016, Prodinger et al., 2011). Among specialized brain cells, astrocytes and microglia are important in immune CNS reactions. There are close interactions between blood macrophages and CNS microglia. Physiological turnover of perivascular macrophages has been demonstrated with the progression of blood-derived monocytes across the glia limitans. This phenomenon might depend on pathological signals such as chemokine ligand 2, CCL2 induced by axonal injury and irradiation (Mildner et al., 2007).

## 1.2 Innate Immunity and the CNS

Innate immunity differs from adaptive immunity by the immediate responses to antigens or pathogens, with limited specificity and diversity of recognized antigens. Innate immunity is said to have “no memory” because the same responses will be generated upon re-exposure to the same stimuli.

The simplest definition of inflammation is the body’s immune response to eliminate the cause of cell injury, remove dead or harmful cells, and initiate repair. It involves host cells, blood vessels and inflammatory proteins (Mellor, 2012). Inflammation can be harmful to normal tissue depending on local and systemic factors controlling the entire process.

The inflammatory response begins with an innate response whereby local vasodilatation leads to fluid and leukocyte accumulation. This complex mechanism is facilitated by various molecules and chemo-attractants—for example, bacterial products and chemokines that must promote the expression of adhesion molecules, selectins, and integrins on both immune cells and vascular endothelial cells. Here, chemokines and activated complement components are key to create a gradient that can lead to extravasation of peripheral immune cells into infected or injured tissue. Upon arrival at the site of injury, phagocytic cells such as neutrophils and macrophages must identify opsonized and non-opsonized dying

cells, pathogens, and debris. They then deliver antimicrobial molecules, engulf the elements, or kill the microbe through the production of reactive free radicals (e.g., reactive oxygen species or ROS).

Innate immune cells (e.g., dendritic cells, macrophages, and monocytes) possess both surface and intracellular receptors. These innate receptors first respond to pathogens or danger signals within their environment. Pathogen-associated molecular patterns are recognized by different families of pattern recognition receptors (e.g., Toll-like receptors or TLRs, nucleotide-binding oligodimerization-like receptors, and RIG-I-like receptors). TLRs can bind and recognize many antigens, from simple proteins and glycolipids to DNA. They are expressed by all types of glial cells, as well as neurons to varying degrees (Hanke and Kielian, 2011).

Cells of innate immunity of the CNS include blood-derived and resident cells. Neutrophils are the most numerous and powerful innate immune cells. Neutrophils are rarely seen in the CNS except in stroke or severe acute encephalitis. They are considered the first line defense against extracellular and intracellular bacteria. They function as phagocytic cells, secrete lytic enzymes, reactive oxygen species, and neutrophil extracellular traps, activate antigen presenting cells and T-cells and secrete cytokines and proinflammatory mediators. The relationship between neutrophils and neuroinflammation is not well studied. However, they might be implicated in the pathogenesis of multiple sclerosis by releasing inflammatory cytokines like tumor necrosis factor alpha (TNFα) and interleukin-6 (IL-6) and causing BBB breakdown (Pierson et al., 2018). Also, recent reports have shown that neutrophils might play important role in the pathogenesis of subarachnoid hemorrhage (SAH), where their depletion in animal models is associated with decreased complications and improved memory after SAH (Provencio et al., 2016). Eosinophils are particularly helpful in allergy and inflammation, with a special role as anti-parasitic cells. Mast cells are very important in allergy and inflammation. They are able to secrete soluble factors such as histamine, proteases, proteoglycans (heparin), prostaglandins, thromboxanes, and leukotrienes, as well as various cytokines (e.g., TNFα, IL-1 and 6, and interferon

gamma, INF-γ). In the inflamed CNS, mast cells have been found in both multiple sclerosis (MS) and experimental autoimmune encephalomyelitis lesions and can directly cause demyelination and oligodendrocyte death (Medic et al., 2010).

Dendritic cells have a special antigen-presenting role to lymphocytes (Miller et al., 2007, Dietel et al., 2012). They cross the BBB to induce direct immune cell activation within the CNS, involving complex interactions between monocytes, dendritic cells, and lymphocytes with the chemokine ligand 2 or monocyte-chemoattractant protein-1. Particularly important are cells of myeloid origin such as the monocytes, macrophages, and resident microglial cells (Prinz et al., 2011). Monocytes are capable of entering tissues to become macrophages (Bechmann et al., 2005). Tissue-specific macrophages may also arise from the yolk sac (e.g., microglia in the CNS and Kupffer cells in the liver). They are not only antigen-presenting cells, but they also secrete cytokines and chemokines to promote inflammation and recruit other immune cells. They are also phagocytic cells.

Glial cells also play a central role in neuroinflammation. They direct leukocytes and inflammatory cells to the site of injury (Babcock et al., 2006). Whilst microglia are of special importance as inflammation modulatory cells, astrocytes are the most abundant. Besides assuming many functions such as supporting the BBB, assuring structural and metabolic integrity of neurons, and modulating synaptic transmission, astrocytes express high levels of TLR-3 and secrete IL-1, IL-6, IL-10, IL-12, TNFα, and C-X-C motif chemokine CXCL10 (Jack et al., 2005). This indicates that astrocytes are capable of inducing strong inflammatory reactions in response to stimuli.

### 1.2.1 Microglia

First described by Pio del Rio-Hortega (Kitamura, 1973), microglia have many features of tissue-specific macrophages, but they have a ramified morphology, possibly to connect faster with neurons (Rock et al., 2004). Simply stated, they are local sensors of the environment that can communicate with other glial and non-glial cells, as they express several surface and internal receptors across species (e.g., CD14, CD11b, CD45, CD68, EMR1, F4/80, and Iba-1) (Prinz et al., 2011).

Microglia are strongly implicated in the inflammatory process following SAH, which might be harmful or beneficial (Larysz-Brysz et al., 2012). These cells are referred to as resting microglial cells, but they continuously monitor the local environment. Their activation depends on intrinsic and extrinsic factors (Kierdorf and Prinz, 2013). Classically, macrophages eliminate dead tissue and secrete mediators to signal other inflammatory cells to amplify the inflammatory reaction. Their functions are presented in Table 1. In experimental models of SAH, activated microglia up-regulate adhesion molecules on endothelial cells to allow inflammatory cells to infiltrate the subarachnoid space (Lucke-Wold et al., 2016).

Inflammatory cells—especially macrophages and neutrophils—engulf red blood cell products to limit acute damage. These cells can be chronically trapped and degranulated, thus releasing multiple inflammatory factors such as endothelin and oxidative radicals that can generate local and systemic inflammatory responses, causing vasoconstriction and arterial narrowing (Lucke-Wold et al., 2016). Microglia receptors like TLR-4 interact with red blood cell degradation products and high mobility group box protein-1 released by dead cells, leading to downstream activation of NFκβ to produce pro-inflammatory cytokines. Reducing microglia activation may decrease delayed cerebral ischemia (DCI) (Lucke-Wold et al., 2016). Preclinical therapeutics that target endothelial E-selectin (an adhesion molecule for neutrophils and antibodies) preventing its ligation to CD11/CD18 (an integrin at the surface of neutrophils and macrophages) have shown a dramatic reduction of DCI. Targeting receptors on these cells, such as Ly6G/C found on the surface of myeloid lineage cells like neutrophils and macrophages, significantly reduced vasospasm, but there is an increased risk of infection with these potent medications (Lucke-Wold et al., 2016).

Microglia are the subject of extensive research because they have been shown to express various TLRs, and they are effective in pathogen clearance. Microglia are considered immature antigen presenting cells (APCs). In the non-active state, they lack CD80, a co-stimulatory molecule for T cell activation, suggesting that they can be regarded as tolerogenic dendritic cells. This is due to their embryologic origin in the yolk sac, like liver macrophages, or local cues down-modulating their

activity. However, once activated, they can promote the accumulation of blood-derived monocytes (Kierdorf and Prinz, 2013). Some of the chemokines and implicated mediators include CX3CL1 (fractalkine), CD200, and CD47, which act on microglial CX3C chemokine receptor-1, CD200R and signal regulatory protein alpha receptors, respectively and exert a quiescent effect on the microglia phenotype (Hanisch and Kettenmann, 2007). They also can be activated by astrocytes (Sievers et al., 1994).

Activation of microglia, infiltrating monocytes and macrophages is observed in most CNS inflammatory disorders. Upon activation, microglia become amoeboid by retracting their ramifying processes and secreting molecules that are either pro- or anti-inflammatory, depending on the context. During neuro-inflammation, infiltrating monocytes, macrophages, and microglia have distinct responses (Table 2). Like macrophages, myeloid cell plasticity or polarization is another special function attributed to microglia: their activation state can be either pro- or anti-inflammatory. This programming capacity is an essential step for the immune response. Despite the wide range of activation, two phenotypes of macrophages/microglia exist: M1 pro-inflammatory state or the classically activated macrophage and M2 anti-inflammatory state, the alternatively activated macrophages. These can be differentiated based on the expression and secretion of different known pro or anti-inflammatory molecules (Barros et al., 2013). M1 microglia are similar to M1 macrophages in their ability to produce pro-inflammatory cytokines and express co-stimulatory molecules (Durafourt et al., 2012a). Human M2 macrophages are more efficient than M1 cells in phagocytizing opsonized targets (Leidi et al., 2009). M2 microglia are also more efficient compared to macrophages at phagocytizing myelin. In general, these cells are mainly phagocytic while also expressing major histocompatibility complex (MHC) class II and costimulatory molecules to promote adaptive immune responses (Table 2).

## Table 1 Functions of microglia

| Role | Reference |
|---|---|
| Clearance of debris, even in fetal life | (Rock et al., 2004) |
| Support axons and modeling of synapses in healthy brain | (Schafer et al., 2012) |
| Synaptic pruning | (Schafer et al., 2013) |
| Pro-inflammatory responses by secreting cytokines, chemokines, complement proteins, nitric oxide, MMPs, and ROS | (Durafourt et al., 2012b) |
| Anti-inflammatory responses by secreting various growth factors and anti-inflammatory cytokines | (Hu et al., 2012) |
| Neuroregeneration in vitro | (Choi et al., 2008) |

## Table 2 Comparison between M1 and M2

| M1 | M2 |
|---|---|
| Pro-inflammatory | Anti-inflammatory |
| | Dampen immune response and promote tissue repair and remodelling |
| Respond to INF-γ, TNF-alpha, pathogen-associated molecular patterns, and LPS | M2a responds to IL-4, IL-13, M2b responds to immune complexes and TLR ligands, M2c or deactivated form responds to IL-10 |
| Respond to bacterial and viral infection | Respond to parasites, cytokines, and immune cells |
| High level of costimulatory molecules such as CD80 and CD86, as well as MHC II efficient antigen presentation capacity | Secrete IGF-1, neural growth factor, brain-derived neurotrophic factor |
| Upregulation of TLR2, TLR4, Fc-gamma, and CCR7 | Express CD23, scavenger receptors CD163/CD204, mannose receptor CD206, and CD209 (DC SIGN). |
| Produces pro-inflammatory and Th1/17 inducing cytokines, chemokines, nitric oxide, and ROS/RNS | Produces anti-inflammatory cytokines such as IL-10 and TGF-beta |

## 1.3 Adaptive Immunity and the CNS

The adaptive immunity arm of the CNS comprises T and B cells, which need APCs to be activated. First, the APCs engulf the pathogens by endocytosis or phagocytosis. Then the degradation products are charged on MHC within the APC. These complexes come back to the surface to interact with appropriate T cell receptor at the cell surface. CD4 T helper cells interact with MHC II and CD8 T cytotoxic cells interact with MHC I. The activation of T cells involves not only the interaction of MHC-antigen complex with T cell receptor, but there are also costimulatory molecules on the surface of the APC (e.g., CD80/86) that interact with T cells to induce activation like CD28. Also needed are the cytokines secreted from the APC (e.g., IL-12) to skew T cells. T cells will also produce IL-2 following activation.

In general, T cell division does not occur in the CNS; if it happens, it can cause local damage by secreting cytokines. The major leukocytes seen during inflammation of the CNS are lymphocytes and monocytes. In acute neuroinflammation, CD4+ T cells play a major role with three phenotypes—Th1, Th2, and Th17. Microglia can secrete different cytokines affecting T cell phenotypes (e.g., IL-12 leading to the Th1 response, IL-4 and IL-10 leading to the Th2 response, and IL-23 leading to the Th17 response). CD4+ cells are proven to induce inflammation in MS and experimental autoimmune encephalomyelitis (Mars et al., 2011, Zielinski et al., 2012). CD8+ cells are less involved and less studied but proven to cause damage in MS (McFarland and Martin, 2007). Also, more recently, several reports have shown that there is increased number and activation of CD4+ T cells, CD8+ T cells, B cells and NK cells in the CSF as well as the peripheral blood of SAH patients. This indicates that SAH induces leukocyte recruitment and activation (Moraes et al., 2015).

In the normal CNS, APCs (dendritic cells and macrophages) are present in the meninges, choroid plexus, and perivascular spaces (Tian et al., 2012). Neurons usually lack expression of MHC-I, which is why viral-infected cells are generally well tolerated. The MHC-II molecules constant expression is restricted to

microglia, as well as costimulatory molecule expression, so they are thought to be the only endogenous cells that can effectively present antigens to T-helper cells. However, a down-regulation mechanism limits the expression of MHC mainly exerted by neurons that are functionally active on microglia, which is why neuronal damage allows for more expression of inflammatory mediators.

Astrocytes also express MHC-II, but not constantly as opposed to microglia. Astrocytes tend to activate Th2 cells more often than Th1 cells, whereas microglia cells recruit Th1 cells. Astrocytes secrete TGF-β, IL-10, and IFN-β, which have anti-inflammatory functions (Tian et al., 2012).

Variations in the inflammatory response are also important. Immune recognition of CNS antigens is complex. In general, there is tolerance of CNS antigens when they stay inside the CNS. However, immune reactions against CNS antigens can be mounted when:

1. antigens are released to lymphoid tissues;
2. antigens are taken up by professional APCs and efficiently presented;
3. antigens are presented in association with microbial infections that induce costimulatory molecules; or
4. the antigen and a non-self-antigen cross-reacting.

Suppression of immune responses in the CNS is mediated by various factors: direct cell-cell interaction, cytokines, or small soluble molecules. Microglia are considered as sensors of the internal environment because of their ability to interact with neurons through receptors such as CD200, SIRP-α, and the fractalkine receptor, CX3C chemokine receptor-1, to perceive neuronal damage. Neurons and astrocytes secrete anti-inflammatory factors as a neural growth factor, brain-derived neurotrophic factor, neurotransmitters, TGF-β, and small molecules such as prostaglandin E2. These act by either suppressing antigen presentation or lymphocyte functions. The resolution of the immune response can be accomplished by either cessation of activation signals or by signals that prevent further activation and promote cell death. For example, programmed death-1 is a molecule associated with T cells that stop division and secretion, and interacts

with ligands on microglia to prevent further T cell activation. These ligands are also present on astrocytes and retinal pigmented epithelium.

An example of the brain immune control that can be compared with SAH is the relapsing and remitting immune responses seen in the progressive relapsing-remitting form of MS. Proposed hypotheses are:

- large amounts of activated lymphocytes have reached the CNS after an initial event and slowly affect the myelin, or
- the immunosuppression mechanisms of the CNS are declining by either reduced function, decreased TGF-β and IL-10 secretion, or high numbers of CNS infiltration antigen-activated immune cells.

This is also poorly understood. Neurons have some resistance to cytotoxicity, especially to activation of the apoptotic extrinsic pathway. They also express the Fas ligand, which inhibits CD 8+ T cell degranulation causing their death. The barriers to an effective immune response are the BBB, limited lymphocyte traffic to the CNS, poor antigen presentation in the brain parenchyma, and a variety of immunosuppressive controls maintained by neurons and glia.

## 1.4 Immune Responses in Stroke and Brain Hemorrhage

SAH occurs when blood vessels rupture into the subarachnoid space. SAH is considered a form of stroke with brain ischemia. The extent of damage depends on the degree to which cerebral blood flow (CBF) is depressed during the minutes immediately following a SAH. Ischemic cell death is mediated by three major events: increases in intracellular $Ca^{2+}$ concentration, tissue acidosis and nitric oxide and free radical production. Ischemic brain injury is also modulated by inflammation, by induction of immediate early genes, and later by apoptosis (Dirnagl et al., 1999).

A new concept in neuro-immunology is the inflammatory mediators and dysfunction of the neurovascular unit following ischemia-reperfusion. The ischemic inflammatory response includes early (within seconds) focal microglia activation leading to inflammatory cytokine (TNFα and interleukins) secretion.

There is a high expression of TLRs (e.g., TLR2 and TLR4) that recognize endogenous alarmins (damage-associated molecular patterns) to propagate inflammation as shown in stroke models (Arslan et al., 2010, Iwata et al., 2010). Within seconds or minutes after ischemia, neurons depolarize and accumulate calcium, propagate excitotoxicity, and may secrete free radicals or may die later by apoptosis. Astrocytes swell and propagate excitotoxicity. Endothelial cells become activated and upregulate adhesion molecules and matrix metalloproteinases (MMPs), leading to damage to the BBB and entry of peripheral cells into the CNS. Peripherally, there is an increase in the secretion of inflammatory cytokines. Peripheral neutrophilia were found following brain ischemia (Barone et al., 1995, Barone et al., 1991) preceding brain infiltration (Chapman et al., 2009). The degree of this peripheral response has been correlated with infarct size in stroke (Buck et al., 2008)).

The post-ischemic inflammatory response ensues when inflammatory cells (i.e., leukocytes and platelets) cause more damage. The endothelium of the microvasculature becomes prothrombogenic by the pro-adhesive nature of leukocytes and platelets, or by their products that cause vasoconstriction and further leukocyte activation. Neutrophils secrete inducible nitric oxide (NO) synthase, which produces toxic amounts of NO, a target for decreasing damage after a stroke (Iadecola, 2004).

# 1.5 Subarachnoid Hemorrhage

## 1.5.1 Brain anatomy

The skull is a rigid container harboring the brain. Covering the brain are three closely related layers termed the meninges. The dura (rigid matter) is the most superficial layer, composed of multiple layers of collagen. The second layer is the arachnoid. The third layer is the thin pia matter, which is closely adherent to the parenchyma. The pia is separated from the arachnoid by the subarachnoid space, which is enlarged at different locations to yield cisterns harboring vessels, nerves,

and cerebrospinal fluid (CSF). SAH occurs when blood vessels rupture into the subarachnoid space.

## Circle of Willis

Two internal carotid arteries and two vertebral arteries supply blood to the brain. The latter merge to form the unique basilar artery. At the base of the skull, the bifurcation of the internal carotid artery gives the anterior cerebral and middle cerebral arteries. The circle of Willis is formed by these two arteries, the posterior communicating arteries, and posterior cerebral arteries coming from the basilar artery. This vascular structure contains a high blood flow and aneurysms tend to be common in this area of brain vasculature, especially at vessel bifurcations (Figure 1).

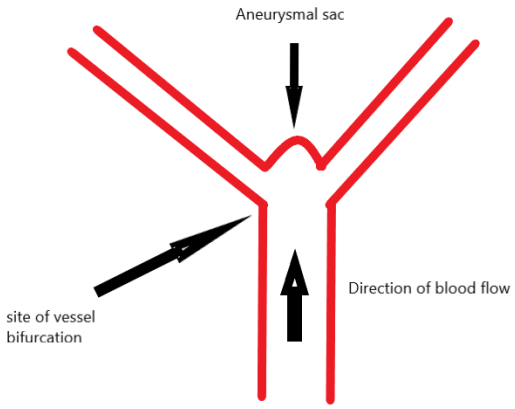


**Figure 1 What is an aneurysm?**

**A s**imple drawing showing the usual site of an aneurysm which is just at artery's bifurcation where hemodynamic stress is elevated.

### 1.5.2 Epidemiology

SAH is an acute cerebrovascular event, whereby blood accumulates in the subarachnoid space. In the neurosurgical world, the term SAH is specifically used to address aneurysm rupture into basal brain cisterns because it is the most dangerous form of SAH. The estimated incidence globally is 9/100,000 persons/year (D'Souza, 2015). SAH is more prevalent in Finland and Japan than in other parts of the world. The most common and important cause of SAH is a ruptured arterial aneurysm (75–85% of cases) (van Gijn and Rinkel, 2001). Less important causes are trauma, use of vasoactive medications, vascular malformations other than aneurysms, vasculitis, and idiopathic causes.

### 1.5.3 Pathophysiology

The pathophysiology of SAH is complex and hard to encompass. In general, it can be divided into aneurysm development, augmentation in size, and rupture, in addition to the mechanisms of brain damage following the hemorrhage. Aneurysms are either saccular, fusiform, blister or complex. Fusiform aneurysms may be formed after arterial dissections. Little is known about what predisposes some patients to form and rupture aneurysms. Risk factors for formation and rupture of intracranial aneurysms include hypertension, smoking, and female sex. Risk factors specific to aneurysm formation are chronic alcohol intake, having a first-degree relative affected, and an inherited disease (e.g., polycystic kidney disease, Marfan syndrome, neurofibromatosis 1, Ehlers-Danlos syndrome, and fibromuscular dysplasia). Risk factors specific for rupture include Japanese and Finnish descent, cocaine abuse, posterior circulation, and large size aneurysm (D'Souza, 2015).

Several theories have emerged as to why cerebral aneurysms form, grow and rupture. Inflammation is strongly implicated in the process (see Section 1.6). The widely accepted high wall shear stress theory (Meng et al., 2007) states that aneurysms form at points of hemodynamic stress, such as arterial bifurcations. Shear stress forces weaken internal elastic lamina, damage medial smooth muscle

cells, and reduce fibronectin of the arterial wall, leading to aneurysm formation. However, this theory fails to explain why aneurysms rupture (Meng et al., 2014). Another important theory is endothelium dysfunction, based on evidence of endothelial cell loss, inflammation, and remodeling implicating mainly MMPs (Kadirvel et al., 2007). It is thought that an endothelial dysfunction is an early event in the biology of aneurysm formation. Whether genetics play a role is uncertain, but a higher incidence in patients with an affected first-degree relative suggests a genetic origin (Ruigrok and Rinkel, 2008). Aneurysms usually grow by either wall proliferation or distention from excessive hemodynamic pressure (Frosen et al., 2012).

SAH occurs after all vascular self-defense mechanisms have failed. There is increasingly strong evidence that SAH causes brain damage in a temporal fashion. In addition to the direct toxic effect of blood products on the parenchyma is the concept of early brain injury (EBI), generally defined as the acute insult to the whole brain within 72 h following the onset of hemorrhage (Fang et al., 2016). The pathophysiology of EBI includes direct mechanical effects on the parenchyma, high intracranial pressure (ICP), decreased cerebral perfusion pressure (CPP), neuroinflammation, brain edema, BBB disruption, and cell death or apoptosis. There are insufficient data in humans to measure the degree of ICP elevation, but experimental trials suggest that high ICP after the hemorrhage is an important pathology leading to ischemia by various mechanisms. Ischemia is usually global and is multifactorial in origin. At the vascular level, there may be some form of circulatory arrest caused by high ICP and/or micro-thrombosis due to platelet aggregates. The result is decreased CPP and CBF leading to ischemia. CPP is defined as the force driving blood into the brain and the CBF is defined as the amount of blood delivered to brain cells per minute. The presence of hydrocephalus and tissue destruction or local delayed cerebral ischemia (DCI) aggravates this ischemia. Disruption of BBB and brain edema are major early events, the major processes involve degradation of collagen in the basal lamina of blood vessels, apoptosis of endothelial cells, and a decrease in tight junction proteins (Sehba et al., 2004).

Ischemic neuronal death or injury is also an important event in the pathophysiology of SAH. Mechanisms involved include the direct effects of neurotoxic blood breakdown products such as hemoglobin, bilirubin, and free radicals. Indirect mechanisms are also implicated such as excitotoxicity, increase in intracellular calcium, energy depletion, anaerobic glycolysis, decreased mitochondrial respiration, proteolysis, lipid peroxidation, and decreased protein synthesis (Sehba and Bederson, 2013). Apoptosis is also an important mechanism of cell death during EBI (Yuksel et al., 2012). Evidence supports the use of anti-apoptotic strategies to decrease or alleviate EBI in SAH, but these are still experimental (Zhang et al., 2016).

Another important mechanism of EBI is endothelial cell dysfunction with subendothelial exposure of collagen, platelet aggregation, activation, and ultimately thrombosis or constriction and ischemia. This is additive to the proposed low level of nitric oxide caused by the presence of hemoglobin.

Secondary complications are very complex and involve a mixture of DCI changes at the level of microcirculation, brain parenchymal changes, and neuroinflammation (Rabinstein, 2011, Rinkel and Algra, 2011, Wong and Poon, 2011, Macdonald, 2014). Of critical importance is DCI which is defined as a focal neurological deficit attributable to a detected vascular territory of intracranial arterial narrowing, angiographic vasospasm, in the absence of alternative causes. It usually occurs after 72h from the onset of SAH (Lee et al., 2018). The mechanisms responsible for DCI are a loss of BBB integrity from EBI, micro-thrombosis, initial brain edema, loss of cerebral autoregulation and cortical spreading depression. This represents a wave of depolarization that propagates through gray matter at 2–5 mm/min and depresses the electroencephalogram activity, causing ischemia.

The term neuro-inflammation is used specifically to refer to activation of resident microglia/astrocytes, the infiltration of systemic immune cells, and the production of chemokines, cytokines, and extracellular proteolytic enzymes and ROS (Mracsko and Veltkamp, 2014).

Lymphatic drainage blockage is an important mechanism of secondary brain ischemia following SAH (Sun et al., 2011). This is currently being actively evaluated after the recent discovery of a CNS lymphatic system (Louveau et al., 2015). Clearance of lymphatic content is weakened in the presence of stroke or SAH (Luo et al., 2016).

### 1.5.4 Morbidity and mortality

Aneurysmal SAH can be fatal. The in-hospital mortality depends on age, loss of consciousness at the ictus, the Glasgow Coma Score at admission, aneurysm size, Acute Physiology and Chronic Health Evaluation II (APACHE II) score, and amount of extravasated blood clot seen on computed tomography (CT) scan (Fisher grade). Mortality rates range from 18% in low-grade SAH to 70% in high-grade SAH (Lantigua et al., 2015). Most deaths occur within 48 h after hemorrhage (Sehba and Bederson, 2013) and are due to the primary hemorrhage in 55% of cases. The rest of the deaths are due to rebleeding and medical complications such as hypotension, pulmonary and cardiac events. Recently, modulating the EBI is a major target to prevent bad outcomes. The overall mortality reaches up to 30%. Feared complications are DCI, cognitive decline and long-term functional deficits in sensorimotor behavior in a relatively young and active population of patients. The risk of dependence on others measured by the modified Rankin Score (mRS) reaches 20% (Rivero Rodriguez et al., 2015). These functional deficits are consequences of second hemorrhage, hydrocephalus, and DCI (Luo et al., 2016).

## 1.6 Inflammation and Subarachnoid Hemorrhage

Recently, multiple studies have highlighted the role of inflammation in SAH, affecting patient outcomes. Unfortunately, most treatments are ineffective against the acute or early brain insult after SAH.

The clinical cardinal signs of inflammation are hotness, redness, swelling, pain, and loss of function, all of which can be clinically observed after SAH. Inflammation after SAH can be viewed as part of the immune response of the CNS

to hemorrhage. An extensive body of evidence supports systemic and local inflammation following SAH (Table 3). Peripheral inflammation not only indicates an inflammatory reaction in the brain but a systemic inflammatory reaction, which is associated with EBI and worse clinical outcomes. Fever is a consequence of SAH associated with increased mortality (Wolf, 2013). Human studies have confirmed high plasma levels of inflammatory cytokines, especially C-reactive protein, IL-6, and IL-10, and that the degree of elevation could reflect the severity of EBI (Zhong et al., 2017). Evidence that inflammatory cytokines like IL-1β, IL-8, and tumor necrosis factor alpha are implicated in systemic or local inflammation following SAH comes from multiple experimental animal models and human trials (Lucke-Wold et al., 2016). According to these studies, pro-inflammatory mediators are associated with the development and degree of DCI following hemorrhage and outcomes of patients. Initially, and importantly for the recruitment of systemic immune cells, proteases such as MMP-9 are thought to be responsible for the degradation of tight junctions to break the BBB. Adhesion molecules (intercellular adhesion molecule-1, vascular cell adhesion molecule-1, and E-selectin), which contribute to inflammation by promoting adhesion of neutrophils, monocytes, and lymphocytes to the endothelial membrane, are expressed in cerebral arteries within 24 h after SAH and correlate with the development of DCI (McBride et al., 2017). E-selectin is linked to the development of DCI in animal models and its inhibition decreased it. In animal studies, inhibition of inflammation decreased brain edema by decreasing disruption of BBB. In humans, an increase in CSF levels of adhesion molecules was observed during the first 72 hours after SAH (Lucke-Wold et al., 2016). Even the disruption of CSF flow following SAH is thought to be partly due to inflammation by alteration of the lymphatic system (Luo et al., 2016).

**Table 3 Specific SAH induced systemic inflammatory responses**

| Response | Effect |
|---|---|
| Elevated levels of circulating cytokines | Major effectors of the systemic inflammatory response |
| Endothelial activation and dysfunction | Smooth muscle changes and DCI |
| Activation of complement and coagulation cascades | Thrombosis and impaired microcirculatory flow |
| Fever | Worse outcome and increase mortality and DCI |
| High respiratory rate | |
| High heart rate | |
| Leukocytosis (elevated WBC count) | DCI and unfavorable outcome |
| High level of catecholamines | Myocardial stunning, pulmonary edema, activating systemic immune responses |

Many local and systemic inflammatory mediators have been correlated with DCI (Table 4). For example, endothelin-1 is found in the CSF of 46% of SAH patients. This can be a cause of vessel narrowing and DCI (Miller et al., 2014). These inflammatory players are not only found in the CSF and or serum, but also in the vessel wall harboring the aneurysm. Innate immune cells have been implicated in cerebral vasospasm following SAH. The presence of abundant neutrophils in the CSF after SAH is an independent risk factor for the development of cerebral vasospasm. In animal models, DCI is shown to have detrimental outcomes after SAH. Important secondary outcomes in SAH patients include hemorrhage, hydrocephalus, and DCI. Neuro-inflammation plays a role in the development of these outcomes (Luo et al., 2016). Inflammation is thought to be implicated in acute and chronic neuronal injury following SAH (Lucke-Wold et al., 2016). Although neuronal death or dysfunction occurs early after SAH due to direct

destruction of blood, necrosis, apoptosis, autophagy, or phagocytosis, late neurological deterioration due to neuronal cell loss is also associated with inflammation and DCI (Macdonald, 2014).

**Table 4 Delayed Cerebral Ischemia and Inflammation**

| |
|---|
| Systemic inflammatory response syndrome is associated with more DCI |
| Inflammatory cells are seen in walls of vasospastic arteries |
| Changes in smooth muscle cells by endothelial activation and cytokines |
| Activated cells such as leukocytes release vasoconstrictors such as endothelin-1 |
| Use of talc, lipopolysaccharide to induce vasospasm |
| Intracellular signaling pathways such as mitogen-activated protein kinase and nuclear factor Kappa-B are important in DCI |
| Nuclear enzymes such as poly (ADP-ribose) polymerase inhibition decreases DCI in animals |

## 1.7 Importance of MFG-E8

Microglial activation plays a pivotal role in EBI following SAH (Fang et al., 2016). Activated microglia can synthesize and secrete pro-inflammatory cytokines (e.g., IL-1β, TNF-α, IL-6, and IL-8). They also secrete MMP-3 and MMP-9, which can worsen ischemic injury (Kawabori and Yenari, 2015). One study showed extensive activation of microglia at day 7 post-experimental SAH in the perivascular cortex and subcortex, preferentially adjacent to the ventricles with high expression to TLR-4. Also, the higher number of activated microglia was associated with more neuronal loss (Luo et al., 2016). The proposed mechanism is that activated microglia can phagocytize both dead and viable neurons, probably through phosphatidylserine/vitronectin interaction (Neher et al., 2013). Also, few human studies have shown that microglia are implicated in DCI. Activated microglia are significantly increased between day 5 and 15 after SAH and are

associated with an increase in amyloid precursor protein, a marker of neuro-axonal injury. They also exhibit upregulation of receptors and cytokine genes for IL-6 and TNFα, and their depletion leads to a decrease of neuronal death after SAH (Schneider et al., 2015). Finally, the microglia phenotype depends on the state of polarization, pro-inflammatory (M1) or anti-inflammatory (M2), which in turn depends on the cytokines present in the local microenvironment. The effect of microglia activation in acute stages as SAH is usually harmful; it is hypothesized that they might be the source of high levels of IL-6 in CSF of SAH patients, a major pro-inflammatory cytokine linked with patient worse outcomes (Schneider et al., 2015).

An important recent advance is the discovery of the MFG-E8 protein, also called lactadherin, a membrane glycoprotein that is implicated in phagocytosis of apoptotic cells. Recently, our laboratory published results regarding the role of MFG-E8 in decreasing kidney inflammation through modulation of the inflammatory response (Brissette et al., 2016). In the brain, MFG-E8 is thought to regulate phagocytosis of viable neurons during neuroinflammation by forming a bridge between activated neurons and phagocytic cells via $\alpha_v\beta3$ and $\alpha_v\beta_5$ integrins and phosphatidylserine. MFG-E8 has neuroprotective effects in ischemic brain disease through different mechanisms including reduction of oxidative stress (Liu et al., 2014) and modulation of the microglia activation into a more anti-inflammatory phenotype. It can be a therapeutical target or agent in the future, especially in SAH.

## 1.8 Clinical Implications and Advances in SAH Research

Inflammation has been shown to be an independent factor for bad prognosis in SAH for the last 50 years (Walton, 1952) and we know that febrile patients do worse (Oliveira-Filho et al., 2001). The inflammatory burden is associated with worse outcomes after SAH (Dhar and Diringer, 2008). The most clinically reported significant prognostic factors for long-term outcomes in SAH patients are age, grade at presentation, clot thickness, and aneurysm size (Lo et al., 2015).

However, many papers found that leukocytosis was associated with an increased risk for developing DCI after SAH and for worse outcomes (Da Silva et al., 2017) (Jelena et al., 2015). Moreover, in a study, a serum leukocyte counts greater than 15 x $10^9$/L was independently associated with a 3.3-fold increase in the likelihood of developing DCI (McGirt et al., 2003).

In clinical practice, there is a continuous need to improve management strategies to fight different diseases. Multiple clinical studies have shown that prevention and treatment of DCI and treating the aneurysm is usually insufficient to improve clinical outcomes in patients with SAH. The only medication widely used for the prevention of DCI is nimodipine; it clinically does not prevent radiologic vasospasm but improves outcomes (Rabinstein, 2011). Thus, new explanations are needed to understand better the pathophysiology behind this common disease.

For example, the mitogen-activated protein kinase (MEK1/2) pathway regulates multiple contractile receptors and may be a viable target for treatment (Lucke-Wold et al., 2016). In preclinical models, multiple strategies have been used to target specific cellular sites to reduce inflammation following SAH (e.g., MEK1/2, CD11-CD18, lymphocytes antigen 6 complex locus G6D, E-selectin, peroxisome proliferator-activated receptor gamma, erythropoietin receptor, N-methyl-D-aspartate receptor, glutamate receptor, amine oxidase enzyme, Sphingosine-1-phosphate receptor, Antithrombin III, IL-1 receptor, endothelin receptor, as well as general inflammation and cytokines). However, very few were translated into clinical studies.

Human trials continue to search for targets to treat SAH. Important trials (de Oliveira Manoel and Macdonald, 2018) used specific molecules as Anakinra, Clazosentan, and erythropoietin to target the IL-1, endothelin, and erythropoietin receptors, respectively, to improve DCI, reduce inflammation, and improve outcomes. Medications such as mitogen-activated protein kinase pathway inhibitors and Tamoxifen have shown promise (Lucke-Wold et al., 2016). Medications are being studied that target peripheral immune cells, preventing their adhesion and blood vessel infiltration. Even medications that are used for other purposes such as heparin, an anticoagulant, and glyburide, used for diabetes, have

anti-inflammatory functions and are being studied in animal models of SAH. However, because we are not fully understanding all EBI events leading to DCI, it is difficult to identify a drug that will improve the outcome of SAH patients. However, investigating the role of inflammatory cells in EBI represents a promising research area.

# 2. Hypotheses, Aims and Objectives

## 2.1 Hypotheses, Aims and Objectives

The hypothesis is that after SAH, inflammation is responsible for neuronal cell damage and worse patient outcomes. This work aims to characterize the type of inflammation that is evoked following SAH. Is inflammation induced after SAH important in the neuronal cell loss and, hence, the undesirable clinical outcomes observed in SAH patients? And, if so, is there any potential role for MFG-E8 in modulating the immune response? My work is a small part of a large, ongoing project characterizing inflammation in an experimental SAH animal model while considering the presence or absence of MFG-E8. This master thesis represents a small part of a larger project in our translational immunology laboratory seeking to understand the mechanisms of inflammation in patients with SAH, from clinical aspects to molecular characteristics governing the activation of inflammatory cells and molecules.

This work is presented in two parts: 1) Using an animal model of SAH, the objectives were to investigate if neuronal damage occurs using different histological techniques. Also, we wanted to see if microglia/macrophages are present and activated after subarachnoid hemorrhage. 2) Using patient charts, the objective was to determine if there were differences in the nature of systemic leukocytosis (and differential leukocyte subsets) and long-term outcomes in SAH patients treated with two standard treatment modalities, surgical clipping or endovascular embolization, that are known to have different effects on the systemic inflammatory response. Patient outcomes were measured using the Modified Rankin Scale (mRS) score, a widely used and clinically proven outcome scale.

# 3. Experimental laboratory Methods

## 3.1 Mice

Male (n = 37) and female (n = 22) donor and recipient C57BL/6J mice of 20-30 g weight from Jackson Laboratory were used for the surgical experiments to obtain slides for staining, collect blood and measure biomarkers as well as phenotyping (Table 5). I worked on the slides for staining. Mice were either MFG-E8 wild-type (WT) or knock-out (KO). The MFG-E8 KO mice of the same C57BL/6J background were obtained from Professor Nagata's Laboratory (Laplante et al., 2017) and were knocked out by creating a mutation in the MFG-E8 gene by using a neomycin cassette to replace exons 4-6 of the gene. The surgery described in subsection 3.2 was performed, injecting either saline (sham) or blood (SAH), on mice to obtain slides. Mouse handling and treatment were under the regulation of the 'Comité Institutionel de Protection des Animaux du Centre Hospitalier de L'Université de Montréal (CIPA)', protocol number N13010JFCs.

## 3.2 SAH and sham surgeries

The prechiasmatic cistern SAH model was used where a donor's blood is injected directly into the prechiasmatic cistern of the recipient mouse. This model is well described in the literature (Sabri et al., 2009). The procedure implies anesthetizing the recipient mouse with 2% Isoflurane gas until it becomes nonresponsive to painful stimuli and to maintain anesthesia. Buprenorphine (0.05mg/kg) is given subcutaneously to decrease peri-procedural pain. Saline 0.9% (5 ml/kg) is also injected subcutaneously to prevent deshydratation. The eyes are covered with a moisturizing ointment. The animal's head is fixed in a stereotaxic frame. The temperature is monitored using an intrarectal thermometer. The oxygen level is monitored using a saturo-meter. The mouse is put on a heated mattress to prevent hypothermia. After assuring that positioning is adequate and the mouse is comfortable, hair over the operative site is shaved using a clipper. The area is

cleaned with a chlorhexidine swap. The donor mouse is anesthetized with 2% Isoflurane gas to be ready for cardiac puncture once the entry hole is drilled in the skull of the recipient mouse. Then, using a #23 scalpel blade, a 1 mm longitudinal incision over the midline at the bregma is made on the prepared area over the head of the recipient mouse. Next, a small hole in the skull just 1-2 mm in front of the bregma is made using a small tipped hand-held drill. The angle of the drill is 40 degrees to the surface of the skull to facilitate injection of blood in the appropriate direction. Intracardiac puncture is done to withdraw 120-200 µl from the donor mouse. 100uL of blood is then injected into the prechiasmatic cistern of the recipient mouse using a spinal needle. The injection is done slowly over 15 seconds. The incision is closed and the animal is allowed to recover from anesthesia. The peri-procedural pain is controlled by an appropriate dose of Acetaminophen (0.16mg/g). In contrast, in the sham group, 100 µl of sterile saline was injected using the same procedural protocol. Mice were killed at 3, 5- or 7-days post-procedure. Just before euthanizing, the heart is exposed and directly injected with a 20 ml saline solution and then a 20 ml solution of 4% PFA. Next, the mouse is decapitated and the brain is extracted carefully from the skull with the help of scissors.

**Table 5 Mice used to obtain slides. Total of 59 mice including donors and recipients used to conduct staining testing and experiments**

| DAY euthanized after surgery | SHAM | SAH |
|---|---|---|
| DAY 3 | 6 KO | 5 KO |
| DAY 5 | 12 KO | 24 (14 KO, 10 WT) |
| DAY 7 | 5 (3 KO and 2 WT) | 7 (3 KO and 4 WT) |

## 3.3 Brain slides preparation

The recovered brain is put in a plastic cryomold, Tissue Tek #4566 (15mm x 15mm x 15mm) with an optimal cutting temperature (OCT) cytoprotective

embedded medium, Tissue Tek #4583 on dry ice. The bloc is preserved at -80°C. Then, these brains were either cryo-sectioned, fixed with acetone and kept frozen or were fixed with paraffin. The paraffin-embedded tissue slides were used for Fluoro-jade staining. The slide's thickness was 7-25 µm depending on the fixation method. There was an average of 5 sections per brain.

## 3.4 Quantification of neuronal damage and Inflammation

Basic, as well as advanced staining techniques, were used to look for and quantify the damage resulting from the SAH (Table 6). Hematoxylin and eosin (H and E) staining was used to confirm the presence of blood and the degree of inflammation, as well as gross damage, if present. This staining technique is used by pathologists as the gold standard to look for infiltrates and necrosis. Sectioned brains were also examined to characterize:

1. Neuronal cell death or dying neurons by Fluoro-jade B staining.
2. Apoptosis by the terminal deoxynucleotidyl transferase dUTP nick end labeling (TUNEL) assay.
3. Inflammation by the number of macrophage/microglia positive for F4/80 staining.
4. Inflammation by the number of neutrophils positive for myeloperoxidase (MPO) staining.

**Table 6 Number of mice used for each staining**

| Mouse | H and E | Fluoro-jade | TUNEL | Macrophage/Microglia activation | MPO |
|---|---|---|---|---|---|
| Sham | | | 3 | 9 | |
| WT | 0 | 3 | | | 1 |
| KO | 3 | 3 | | | 1 |
| SAH | | | 3 | 9 | |
| WT | 0 | 3 | | | 1 |
| KO | 4 | 3 | | | 1 |

### 3.4.1 Hematoxylin and eosin (H&E) staining

H&E staining was performed on brain slides by the molecular pathology platform at CRCHUM. The light microscope (Nikon Eclipse E600) was used to visualize the staining at 2x and 10x magnifications. 3 pictures were taken around each lateral ventricle for a total of 6 periventricular pictures per brain slide. A blinded pathologist was in charge of the evaluation regarding any gross blood, infiltrates and/or necrosis.

### 3.4.2 Immunofluorescence staining (IF)

The anti-neuronal nuclei (NeuN) clone A60 monoclonal antibody (Millipore #MAB377) was used with a concentration of 1/25 to stain specifically mature neurons. The secondary antibodies used were either AF 488 donkey anti-mouse or AF 594 donkey anti-mouse (ThermoFisher Scientific #A21202 LT and #A21203 LT, respectively), depending on the availability. 4',6-diamidino-2-phenylindole (DAPI) was used to stain nuclei (Figure 2). Briefly, the protocol involves taking out slides from -80°C and letting them thaw for 20-30 minutes at room temperature (RT). Then the slides are put for 10 minutes in cold 100% acetone and then for 5 minutes in cold 70% ethanol. Then they are put in PBS (Phosphate-buffered-Saline) 1X solution for 3 minutes at RT. Then they are put in the humidity chamber covered with PBS 1X for 10 minutes at RT. Then another wash with PBST for 2-3 minutes at RT. Then the sections are blocked with 10% serum for 30 minutes at RT. Then the slides are incubated with the primary antibody for 1 hour at RT. Next, the slides are washed in PBST (PBS 1X + 0.05% Tween) 7 times for 2 minutes at RT. Next, they are incubated with secondary antibody for 40-60 minutes at RT. The slides are then washed in PBST again. Then after washing, the slides are dabbed in a mounting medium (DAPI) and covered with a glass coverslip. They are then stored in the fridge at 4°C.

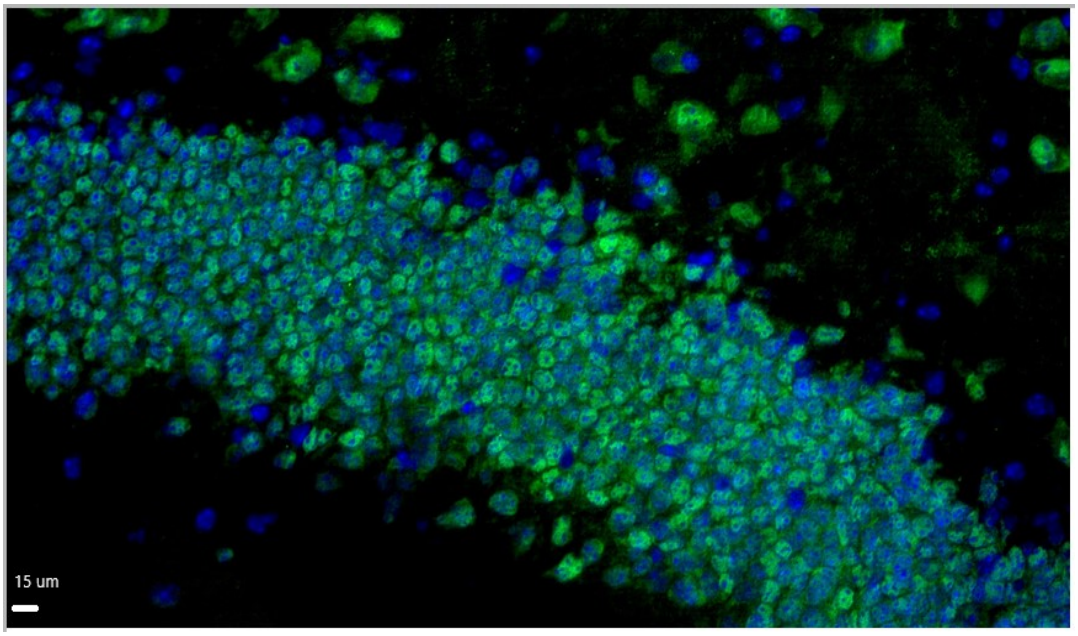


**Figure 2 NeuN staining.**

Magnified image shows mature neurons in the hippocampus area, NeuN (green) and DAPI (blue).

## Fluoro-jade staining and neuronal degeneration

Fluoro-jade is commonly used to stain degenerating neurons in ex-vivo tissues of the CNS. Fluoro-jade B (Millipore) at 0.01% concentration stock solution was used to evaluate for neuronal damage at day 7 after surgery. Briefly, the slides are deparaffinized with xylene and then are fixed with 4% freshly prepared formaldehyde. Then they are rehydrated through a graduated alcohol series. Then they are rinsed with distilled water and potassium permanganate (0.06% KMnO4) was used for background suppression. Next, they are rinsed again and stained with Fluoro-jade in 01% acetic acid for 10 minutes. They are rinsed again in distilled water and then left to dry at 50º for 5 minutes. Then they are covered with a coverslip with mounting media. Three Paraffin-embedded sections of each group were stained (Table 6). The slides were examined with an epifluorescent

microscope (Zeiss Observer ZI) at 450–490 nm excitation wavelength and an emission peak of 520 nm and were counted by a blinded investigator using Image J software. Each brain section was imaged 6 times and then the average number of cells is taken around the periventricular area and the means were calculated. KO and WT groups were compared together.

## TUNEL assay and apoptosis

The TUNEL assay detects DNA fragmentation by labeling the terminal end of nucleic acids. It is used specifically for the detection of apoptosis. The TACS 2 TdT-DAB kit (TREVIGEN #4810-30-K) was used to stain 1 sham and 1 SAH slides at day 3, 5 and 7 respectively according to the manufacturer' instructions. (Table 6). Apoptotic cells were counted in the cerebral cortex, cerebellar cortex, thalamus, hippocampus, and periventricular area. The means were compared between the sham and the SAH groups using a two-tailed t-test.

## Microglia/macrophage

The glycoprotein F4/80, which is expressed at high levels on different types of macrophages, was used to identify the number of microglia/macrophages in SAH vs sham. MCA497G mouse anti-mouse (AbD Serotec) was the primary antibody, and AF 488 rat anti-mouse (ThermoFisher Scientific) was the secondary antibody. The sections used included day 5 frozen sections and day 7 paraffin-embedded slides (Table 6). The counts were done manually.

## MPO staining

MPO is a peroxidase enzyme encoded by the MPO gene and is most abundant in neutrophil granulocytes. It is a lysosomal protein stored in the azurophilic granules of the neutrophil. MPO was used to stain 2 KO females and 2 WT males, 1 sham, and 1 SAH each at day 7. The staining was performed by the molecular pathology platform at CRCHUM according to standard procedures. The count was done manually on light microscopy counting positive cells per 2 brain sections. The average number of cells was compared between SAH and sham in each group.

## Statistical Analysis

Microsoft Excel 2016 version 15.19.1. was used to calculate means, SEM and P values. Treatment groups were compared with a two-tailed t-test or ANOVA and alpha was set at 0.05.

# 4. Results of Experimental Animal Model

The presence of blood in the SAH group was confirmed by H and E staining in all examined slides (Figure 3). Also, there were no infiltrates or gross necrosis in all examined slides.

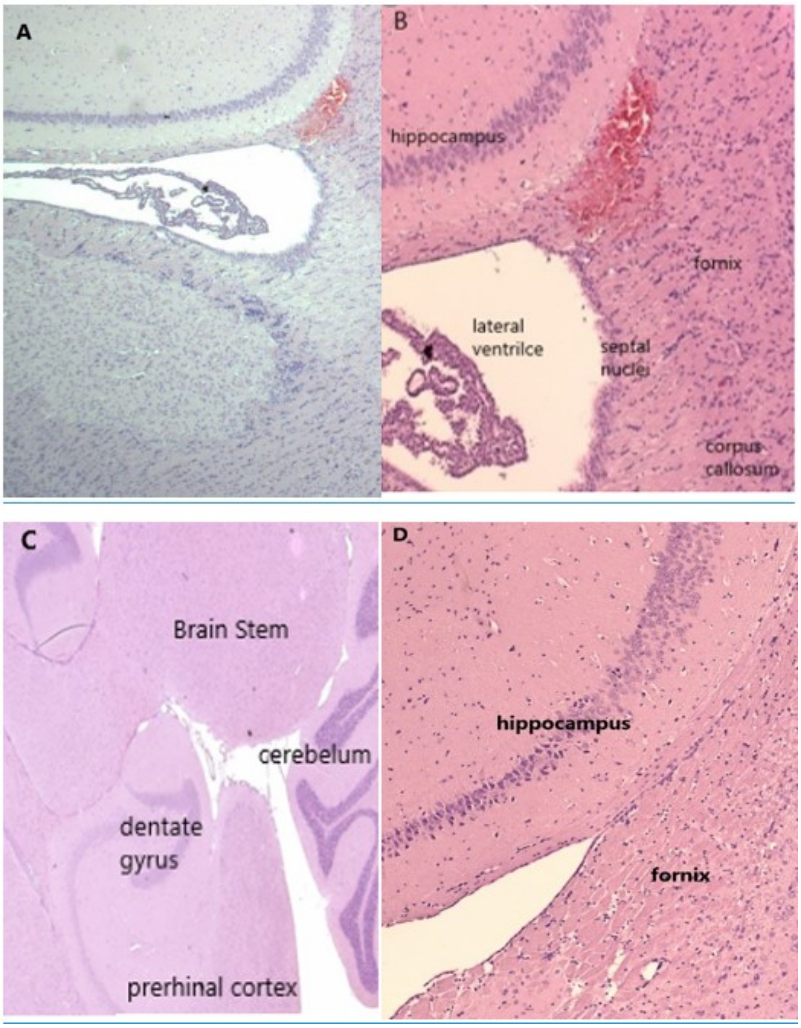


**Figure 3 Blood in SAH sections.**

H and E staining light microscopic images of SAH at 2X (A) and 10X (B) magnification vs sham at 2X (C) and 10X (D) magnification. Both were in KO mice. There is periventricular blood in the subarachnoid space in the SAH (A, B), but not in the sham (C, D).

Using Fluro-Jade (Figure 4) and TUNEL (Figure 5) staining, there were trends for more degenerated neurons in the SAH group than sham group ($p = 0.61$) and more in the KO than WT group. The most degenerated neurons were observed in the KO SAH group but it was not statistically significant when compared with KO sham (*p= 0.53)*, WT SAH (*p= 0.2).*

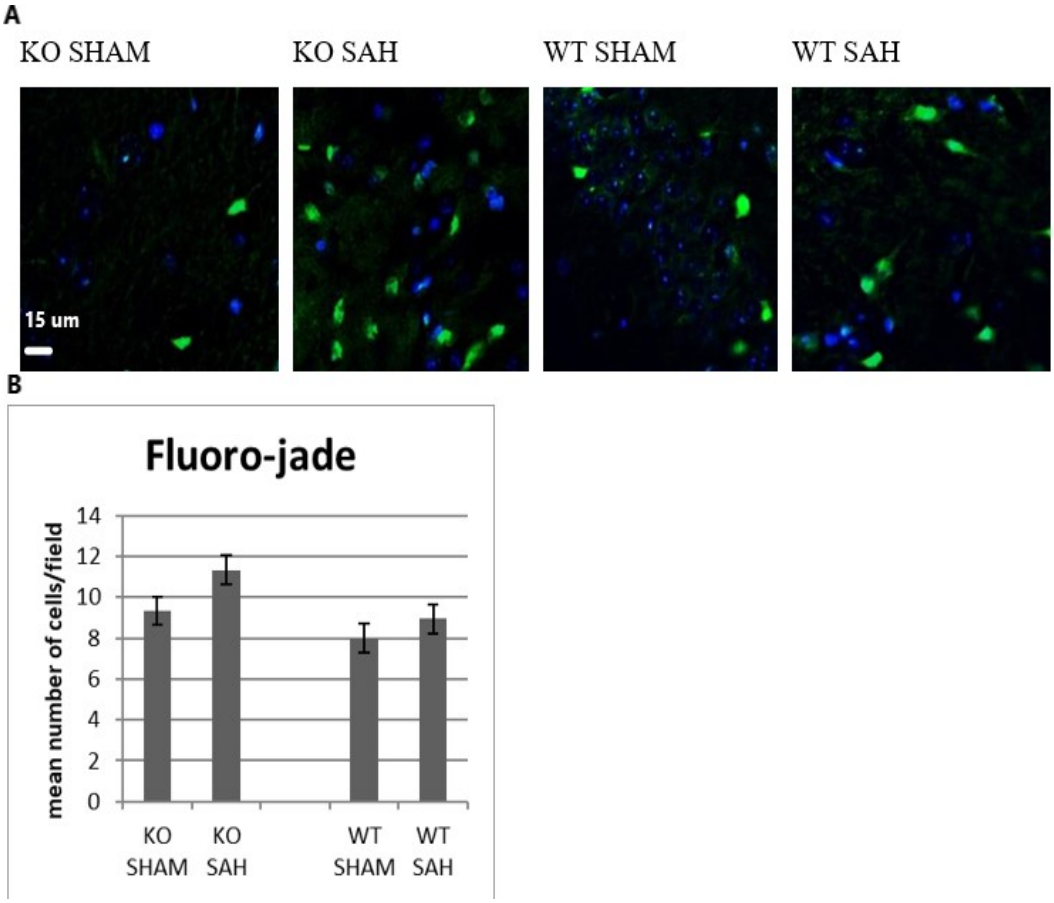


**Figure 4 Trends for More Degenerated Neurons in SAH**

Fluoro-jade immunofluorescence staining of KO or WT SAH vs sham mice (A), degenerated Fluoro-jade positive (green) cells and DAPI (blue) non-degenerated nuclei. (B) The graph shows the mean (±SEM) number of degenerated cells in SAH and sham groups (n = 3). There might be more degenerated neurons in the KO SAH group, ($p > 0.05$ for both comparisons).

The TUNEL assay showed a very weak signal for DNA fragmentation at days 3 and 5 post-SAH. At day 7, on paraffin-embedded sections, there was a small difference between SAH and sham, but the means were not significantly different ($p = 0.49$)

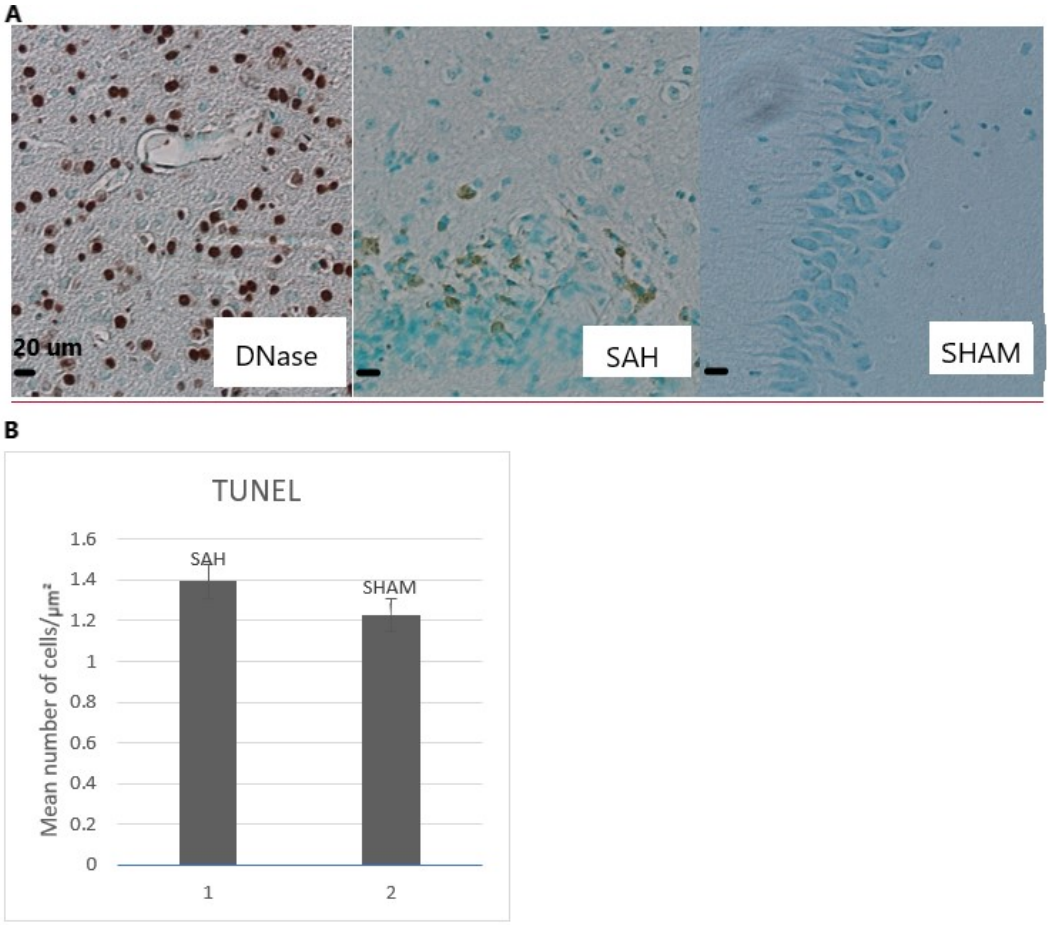


**Figure 5 SAH induces a little more apoptosis.**

(A) TUNEL staining 20x microscopic images of the periventricular/hippocampus area showing apoptotic cells (brown-green). Left picture: Positive control (DNAse-treated), middle picture: SAH and right picture: Sham. (B) Graph of the mean number of cells/ µm² of SAH vs sham showing a trend for more apoptotic cells in SAH mice (n = 2, $p = 0.49$).

**Macrophages and microglia evaluation**

F4/80 was used to measure macrophage numbers. At days 5 and 7 (Figures 6 and 7), there was some evidence of more macrophages/microglia near the cortex in the SAH group than the sham group. However, the mean numbers did not reach statistical significance ($p > 0.05$ and 0.80, respectively).

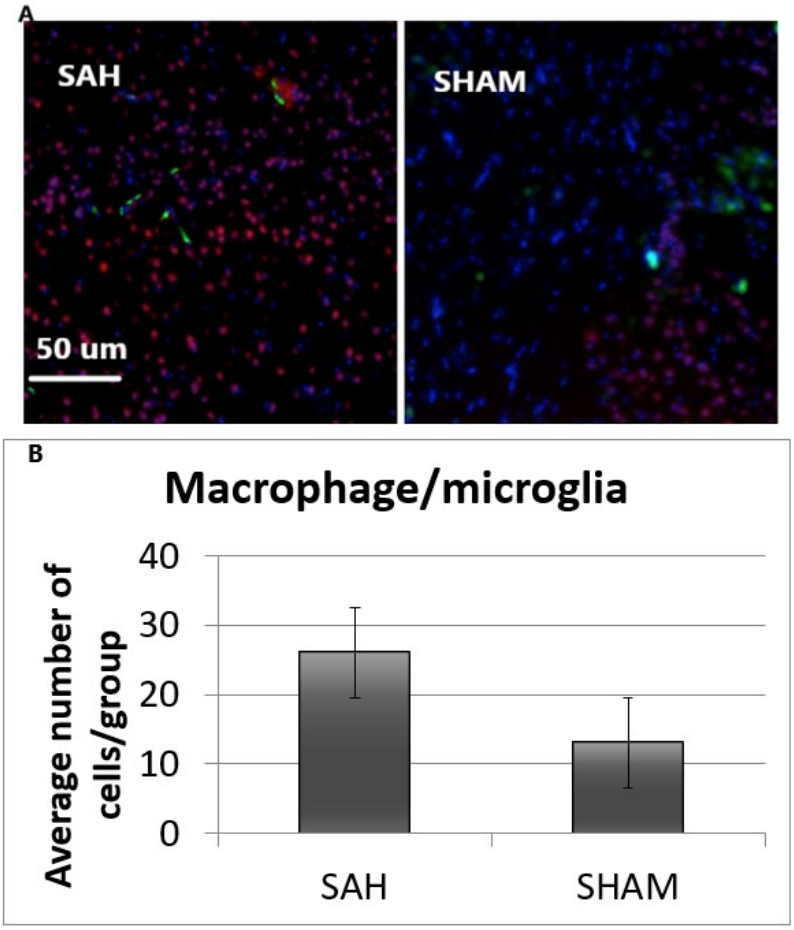


**Figure 6 F4/80 staining Day 5.**

Image shows F4/80 (green) positive cells, NeuN (red mature neurons) and DAPI (blue nuclei). (B) Graph showing the mean numbers of F4/80 positive cells in each group (n = 4). There is a trend for more macrophages/microglia in the SAH group (*p > 0,05).*

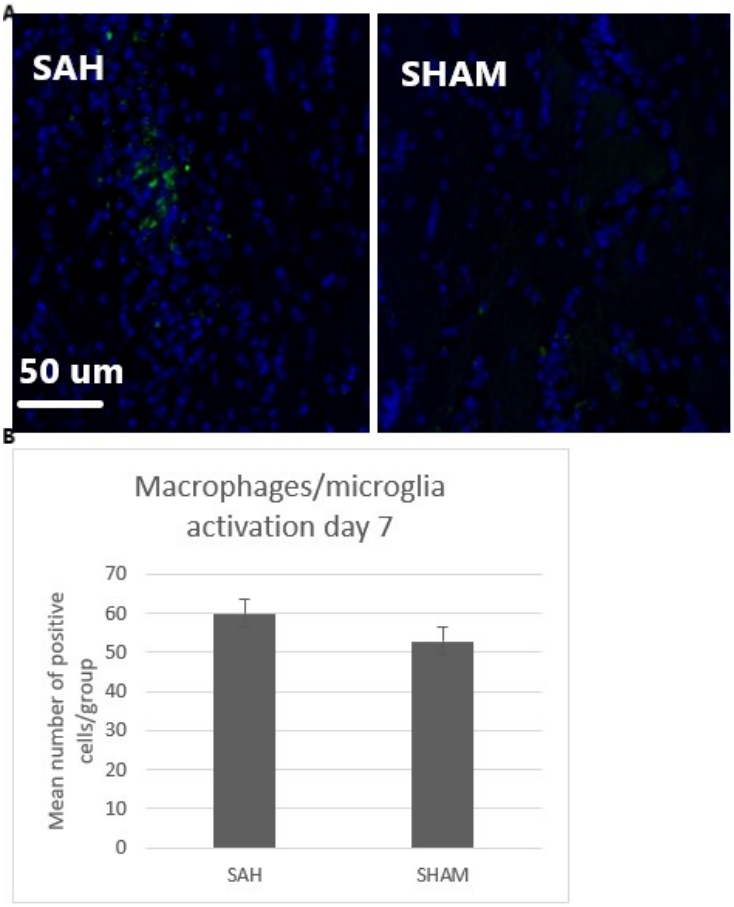


**Figure 7 F4/80 staining Day 7.**

(A) image showing F4/80 (green) positive cells and DAPI (blue nuclei of other cells). (B) Graph showing a trend for more macrophages/microglia in the SAH group (n= 7; *p = 0.08).*

**Neutrophil evaluation**

The number of neutrophils was higher in the SAH group compared to the sham group, as measured by MPO staining. (Figure 8). This was not statistically significant ($p = 0.27$).

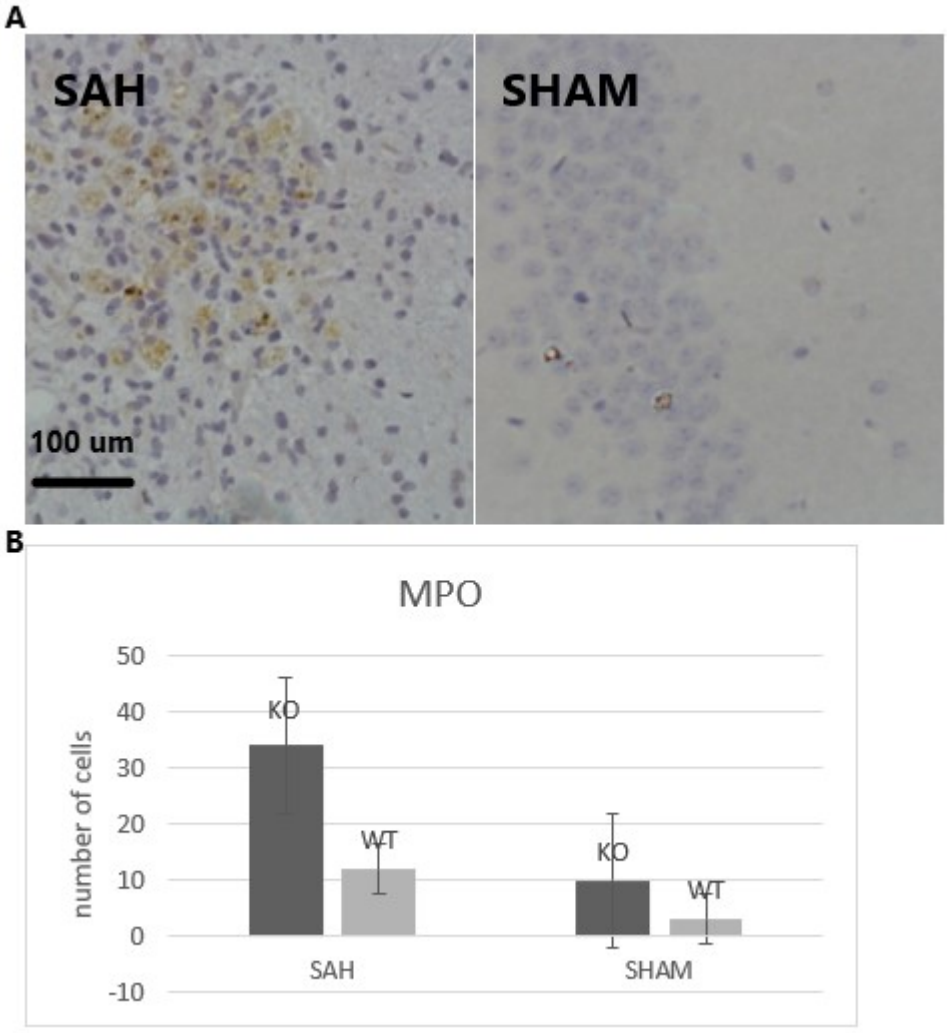


**Figure 8 MPO staining.**

(A) Light microscopic images at 20x showing MPO positive cells (dark brown). (B) Graph showing more neutrophils in the SAH group and more in the KO group (n = 2, $p = 0.27$).

# 5.Clinical Study

## 5.1 Clinical Methods

For the clinical part of the study, data were collected from 100 patients admitted to Notre-Dame Hospital from the Centre Hospitalier de l'Université de Montréal. All patients had been diagnosed with SAH based on clinical symptoms and CT brain scan. The data were divided into demographics, clinical and laboratory parameters for two standard treatment groups (50 patients each): surgical clipping or endovascular coiling. Surgical clipping involves performing an open surgery through the skull and then identifying the bleeding aneurysm, which is secured by applying a metal clip to its neck to eliminate it from the blood circulation. Endovascular coiling is done by catheterization of the femoral arteries usually to be able to access the brain arteries and applying coils to the sac of the aneurysm to secure it. Open surgery is more invasive as it opens the skull and manipulates brain tissue to reach the aneurysm, while coiling is direct into the arteries. Different factors dictate the decision to use one procedure versus the other. These include, but not limited to, age, the presence of comorbidities, clinical status after the hemorrhage, type of the aneurysm, size of the aneurysm amongst other factors.
To assess the severity of disease at admission, the World Federation of Neurosurgery severity scale and the Fisher grade were used (Rosen and Macdonald, 2005) (Tables 7 and 8). All patients were treated within 48 h to prevent rebleeding risk according to the American Heart Association guidelines (Connolly et al., 2012).

**Table 7 World Federation of Neurosurgery Scale**

| Glasgow Coma Score | Motor Deficit | Scale |
|---|---|---|
| 15 | No | 1 |
| 13–14 | No | 2 |
| 13–14 | Yes | 3 |
| 7–12 | Yes or No | 4 |
| 3–6 | Yes or No | 5 |

**Table 8 Fisher Grade**

| Grade | CT scan finding |
|---|---|
| 1 | No visualized blood |
| 2 | Diffuse disposition or thin layer with all vertical layers less than 1 mm thick |
| 3 | Localized clot and/or all vertical blood layers are greater than 1 mm thick |
| 4 | Diffuse or no SAH but with intracerebral or intraventricular blood |

Patients were managed by experienced neurosurgeons, neuro-intensivists, and neurologists. Conditions known to alter immunity were taken into account (e.g., diabetes, hypertension, dyslipidemia, cancer, exposure to chemotherapy or radiotherapy, taking immunomodulatory medications or steroids, and pregnancy). Clinical parameters of relevance for prognosis were collected, such as mean arterial pressure (MAP), MAP at presentation, MAP variations during the peri-operative period, core temperature, and heart and respiratory rate at presentation. Peripheral leukocyte counts with differentials (number of monocytes, neutrophils, lymphocytes, etc) were collected at presentation, between 1 and 3 days after the procedure, and at 5 days post-intervention (or the last value available to reflect the end of the intervention's effect). Other laboratory data examined were creatinine, bilirubin, and hemoglobin levels, platelet counts and hematocrit at presentation, and serum sodium in the peri-operative period. The outcome was measured using the Modified Rankin Score (mRS), which is commonly used for assessing

neurological outcomes (Lahiri et al., 2016) (Table 9). mRS was calculated at 24 h after admission.

## Statistical analysis

Parametric (*t*-test, Analysis of Variance) and non-parametric (Chi-Square) tests were conducted using SAS 9.4 software. For demographic variables, statistics were used and the confidence interval (CI) was set to 95% with *p*-value significant if ≤0.05. A t-test was used to compare two groups of numerical data while Chi-square test was used for nominal data. For peri-procedural variables, such as clinical status and Fisher grade, laboratory data, use of mechanical ventilation, use of steroids or other variables that could affect inflammation, t-test for unequal variances was used together with Chi-square test in order to detect the difference between the two treatment groups. Using ANOVA for analysis of covariance, maximum leukocytosis (approximately 2 days post-procedure) was compared between the two groups. Also, at five days, WBC counts were compared between the two groups. These comparisons are adjusted for WBC counts at admission because analysis of covariance is a preferred way to adjust for the baseline. It must be noted that one WBC value was missing from the endovascular group, 4 differential counts were missing from the surgery group, and 1 differential count was missing from the endovascular group at 5 days post-procedure. These missing data stemmed from difficulties associated with finding information retrospectively from patient charts, or patients were transferred to another hospital after the procedure, making access to files challenging. These missing data were taken into account during the analysis. mRS values were calculated for all but one surgery group patient, who was lost in the follow-up. To measure the effect of changes of leukocyte number on mRS, the interaction between mean changes of WBC counts from baseline at admission and mRS was tested. Logistic regression was made to evaluate the presence of an association between neutrophil-lymphocyte ratio (NLR), monocyte-lymphocyte ratio (MLR), eosinophil-lymphocyte ratio (ELR) and platelet-lymphocyte ratio (PLR) at admission, day 5 and day 10 with odds of poor outcome.

**Table 9 Modified Rankin Score**

| Score | Description |
|---|---|
| 0 | No symptoms |
| 1 | No disability, able to carry out all previous activities and duties but has symptoms |
| 2 | Slight disability, unable to carry out all previous activities and duties but autonome |
| 3 | Moderate disability requires some help but walks without assistance |
| 4 | Moderately severe disability, unable to walk without assistance and unable to attend to own bodily needs without assistance |
| 5 | Severe disability, constant nursing care, bedridden, incontinent |
| 6 | Dead |

# 6. Results of The Clinical Study

## 6.1 Demographic data

The two treatment groups had similar demographic characteristics ($p > 0.172$ among all tests; Table 10).

**Table 10 Demographic variables. SD, standard deviation; CI, confidence interval; F, Female; M, Male; N, Number of patients**

| Variable | Surgerical Clipping | Endovascular Embolization | *p* value |
|---|---|---|---|
| Age (years) | 56 ± 13.34 (mean ± SD)<br>1.14–16.62 (95% CI) | 57.6 ± 11.75 (mean ± SD)<br>9.82–14.65 (95% CI) | 0.38<br>*t*-test |
| Sex | F = 32, M = 18 | F = 33, M = 17 | 0.83<br>Chi Square |
| Comorbidities | *N* = 26 | *N* = 23 | 0.54<br>Chi Square |
| Use of immunomodulators or chemotherapy | *N* = 4<br>Rapamune, sirolimus, azathioprine, chemotherapy, steroid | *N* = 1 methotrexate | 0.17<br>Chi-Square |

## 6.2 Peri-procedural parameters

The two groups did not differ in terms of World Federation of Neurosurgery scale, Fisher grade, use of steroids or antibiotics peri-procedure, and rate of nosocomial infection (Table 11). Inflammatory parameters such as heart rate, platelet count, and hemoglobin concentration were also similar between groups. Na concentration, which is important for prognosis, was also similar between the two groups. Interestingly, surgery was associated with a longer duration of mechanical ventilation than the endovascular embolization group ($p = 0.07$). Only, the MAP at baseline was higher in the endovascular embolization group ($p = 0.026$). Temperature ($p = 0.054$), respiratory rate ($p = 0.005$) and creatinine ($p = 0.001$),

and lactate ($p$ = 0.042) concentrations were higher in the surgical than endovascular embolization group.

**Table 11 Peri-procedural clinical and laboratory parameters. SD, standard deviation; CI, confidence interval; N, Number of patients**

| Clinical parameters | Surgical clipping | Endovascular embolization | $p$ value |
|---|---|---|---|
| Time from SAH to hospital (h) | < 24 (43 patients)<br>≥ 24 (7 patients) | < 24 (38 patients)<br>≥ 24 (12 patients) | 0.20<br>Chi Square |
| World Federation of Neurosurgery Scale<br>1<br>2<br>3<br>4<br>5 | <br>$N$ = 10<br>$N$ = 13<br>$N$ = 9<br>$N$ = 10<br>$N$ = 8 | <br>$N$ = 10<br>$N$ = 14<br>$N$ = 15<br>$N$ = 10<br>$N$ = 1 | <br>0.13<br>Chi Square |
| Fisher Grade<br>1<br>2<br>3<br>4 | <br>$N$ = 7<br>$N$ = 7<br>$N$ = 11<br>$N$ = 25 | <br>$N$ = 7<br>$N$ = 8<br>$N$ = 8<br>$N$ = 26 | 0.90<br>Chi Square |
| Use of steroids or antibiotics peri-procedural, period where WBC counts are analyzed | $N$ = 11 | $N$ = 14 | 0.45<br>Chi Square |
| Infection | $N$ = 13 | $N$ = 12 | 0.81<br>Chi Square |
| Use of mechanical ventilation | $N$ = 25 | $N$ = 32 | 0.16<br>Chi Square |
| Duration of mechanical ventilation (h) | ≤ 48 (0 patients)<br>> 48 (25 patients) | ≤ 48 (21 patients)<br>>48 (11 patients) | 0.07<br>Chi-square |
| MAP base line (mean ± SD mm Hg) | $N$ = 35, 99.95 ± 13.41<br>95.34–104.6 (95% CI) | $N$ = 43, 107.3 ± 19. 6<br>101.3–113.3 (95% CI) | **0.03**<br>$t$-test |
| MAP variation peri-procedure (mean ± SD mm Hg) | $N$ = 41, 17.36 ± 11.66<br>13.68–21.05 (95% CI) | $N$ = 41, 19.60 ± 11.19<br>16.08–23.14 (95% CI) | 0.79<br>$t$-test |

| | | | |
|---|---|---|---|
| Temperature (mean ± SD °C) | *N* = 19, 36.63 ± 0.51 | *N* = 27 36.35 ± 0.80 | **0.05** *t*-test |
| Heart rate (mean ± SD beats per minute) | *N* = 30, 79.8 ± 19.2 | *N* = 39, 79.9 ± 19.9 | 0.842 *t*-test |
| Respiratory rate (mean ± SD breaths per minute) | *N* = 26, 18.54 ± 3.68 | *N* = 28, 17.89 ± 2.08 | **0.01** *t*-test |
| Hematocrite (mean ± SD; 0.41–0.58) | *N* = 40, 0.389 ± 0.043 | *N* = 43, 0.402 ± 0.046 | 0.69 *t*-test |
| Maximum platelet count peri-procedure (mean ± SD; 140–450×$10^9$/L) | *N* = 50, 274.8 ± 107.4 | *N* = 50, 267.2 ± 61.4 | 0.66 *t*-test |
| Minimum hemoglobin peri-procedure (mean ± SD; 120–160 g/L) | *N* = 49, 95.55 ± 15.23 | *N* = 50, 103.2 ±18.1 | 0.23 *t*-test |
| Maximum creatinine peri-procedure (mean ± SD; 53–112 umol/L) | *N* = 50, 79.06 ± 38.99 | *N* = 50, 76.66 ±24.13 | **0.001** *t*-test |
| Lactate peri-procedure (mean ± SD; 0.6–2.4 mmol/L) | *N*=24, 2.41 ± 2.26 | *N* = 30, 2.14 ±1.51 | **0.04** *t*-test |
| Minimum sodium peri-procedure (mean ± SD; 135–145 mmo/L) | *N* = 49, 136.5 ± 3.3 | *N* = 50, 136.9 ± 3.1 | 0.617 *t*-test |

## 6.3 WBC counts

The WBC count data confirm evidence of leukocytosis at admission in patients with SAH, with mean WBC counts of 12.83×$10^9$/L and 14.03×$10^9$/L (normal 4–11×$10^9$/L) in surgical and endovascular groups, respectively (Table 12). Maximum leukocytosis (approximately 2 days post-procedure) was 9% higher in the surgical group ($p$ = 0.014). Also, at five days, WBC counts remained higher in the surgical group ($p$ = 0.029), but they had returned to within normal limits. These comparisons are adjusted for WBC counts at admission because of analysis of covariance, which is a preferred way to adjust for the baseline. The lymphocytes were 30% higher in the embolization group at a maximum period of inflammation around 2 days ($p$ = 0.0005). Post-intervention, there was some rise in monocytes, which remained elevated at 5 days in the surgical group (though not statistically

significant). Other counts were similar between the two groups without clinical significance.

**Table 12 Mean (±SD) WBC counts at different times peri procedure**

| Variable | Surgical clipping | Endovascular embolization | *p* value |
|---|---|---|---|
| WBC at admission ($\times 10^9$/L) (normal 4–11 ($\times 10^9$/L) | 12.83 ± 4.57 | 14.03 ± 4.52 | |
| WBC max | 13.61 ± 4.06 | 12.50 ± 3.54 | **0.01** |
| WBC at 5 days (1 missing endo) | 10.89 ± 4.83 | 9.925 ± 2.748 | **0.03** |
| Neutrophils at admission (%) (normal 40–75%) | 73.98 ± 16.01 | 81.38 ± 12.56 | |
| Neutrophils max (%) | 81.06 ± 13.09 | 80.10 ± 7.67 | 0.55 |
| Neutrophils 5 days (%) | 74.09 ± 9.31 | 75.31 ± 7.99 | 0.97 |
| Monocytes at admission (%) normal (0-12%) | 6.40 ± 2.63 | 4.89 ± 2.35 | |
| Monocytes max | 7.30 ± 3.23 | 6.76 ± 2.10 | 0.69 |
| Monocytes 5 days | 9.06 ± 2.71 | 7.98 ± 3.37 | 0.52 |
| Eosinophils at admission (%) (normal 0–4%) | 0.91 ± 1.21 | 0.5 ± 0.95 | |
| Eosinophils max | 0.42 ± 0.59 | 0.71 ± 1.18 | 0.06 |
| Eosinophils 5 days | 1.72 ± 1.70 | 1.66 ± 3.40 | 0.95 |
| Basophils at admission (%) norml (0-4%) | 0.16 ± 0.23 | 0.01 ± 0.06 | |
| Basophils max | 0.28 ± 1.27 | 0.02 ± 0.07 | 0.13 |
| Basophils 5 days | 0.32 ± 0.43 | 0.19 ± 0.44 | 0.62 |
| Lymphocytes at admission (%) (normal 22-51%) | 18.32 ± 13.85 | 12.76 ± 10.94 | |
| Lymphocytes max 5 missing | 8.89 ± 3.90 | 11.56 ± 5.53 | **0.0005** |
| Lymphocytes 5 days | 14.57 ± 6.86 | 14.32 ± 6.89 | 0.593 |

The most prominent systemic cells in the blood were neutrophils, which remained the highest percentage of cells even at 5 days (Figures 9 and 10).

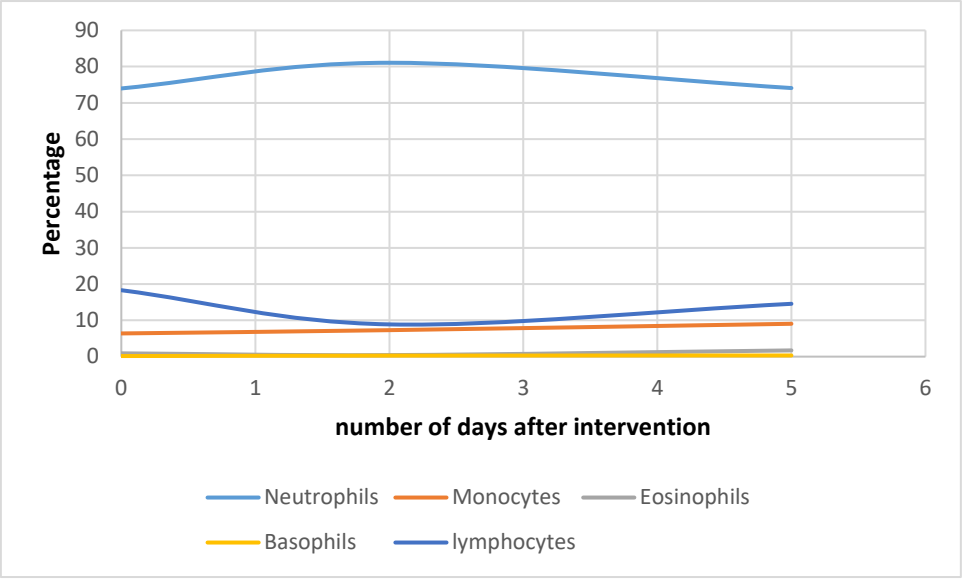


**Figure 9 WBC differential percentages from days 1 to 5 in the surgery group.**

As noticed that neutrophils represent in average 80% of leukocytes in the blood of SAH patients and they remain the predominant cells at 5 days after surgery.

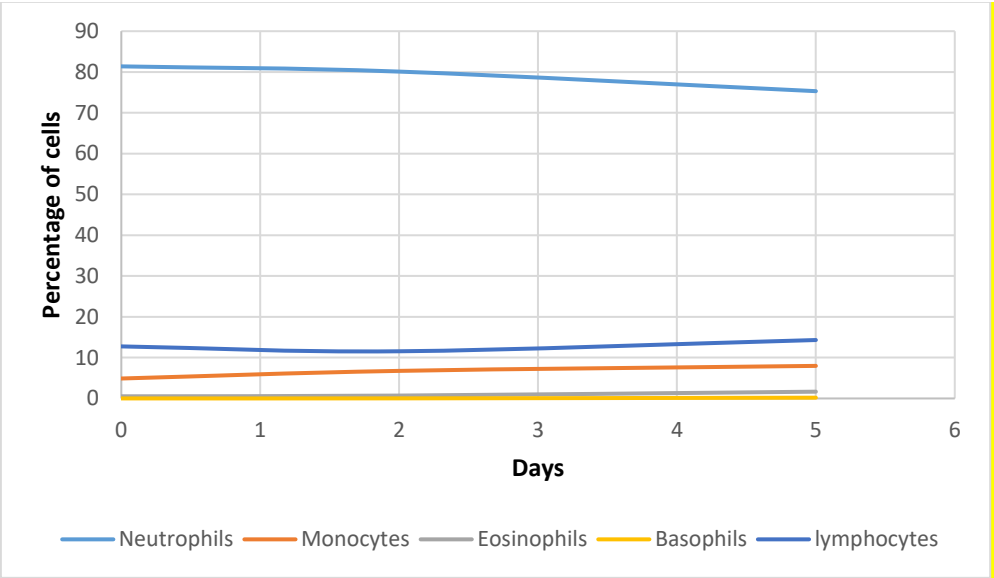


**Figure 10 WBC differential percentages from days 1 to 5 in the endovascular group.**

Neutrophils represent 80% of leukocytes in the blood of SAH patients after endovascular coiling.

### 6.3.1 WBC changes and mRS

Modified Rankin Score (mRS) values were calculated for all but one surgery group patient, who was lost in the follow up (Table 13). The mean follow-up period was approximately 16 and 18 months for the surgical and endovascular groups, respectively. Mortality (i.e., mRS 6) was higher in the surgical (18.4%) than the endovascular group (4.0%). However, worse outcome, defined as mRS 4–6, was similar between the two groups, with no clinical significance (Table 13).

**Table 13 mRS values for surgery and endovascular groups**

| Surgery | Frequency | Percent | Endovascular | Frequency | Percent |
|---|---|---|---|---|---|
| **0** | 5 | 10.2 | **0** | 3 | 6.0 |
| **1** | 13 | 26.5 | **1** | 17 | 34.0 |
| **2** | 15 | 30.6 | **2** | 9 | 18.0 |
| **3** | 4 | 8.2 | **3** | 12 | 24.0 |
| **4** | 2 | 4.1 | **4** | 5 | 10.0 |
| **5** | 1 | 2.0 | **5** | 2 | 4.0 |
| **6** | 9 | 18.4 | **6** | 2 | 4.0 |
| **Total** | 49 | **100** | | **50** | **100** |

Total WBC counts at 5 days were similar between the two groups (Figure 11, Table 14). A negative association existed between neutrophilia and surgery ($p$ = 0.07). Monocytes were decreased at 5 days in all groups at similar rates. Lymphocyte changes differed between groups. None of these observations reached clinical significance when comparing each change with mRS groups of both surgery and endovascular ($p$ = 0.073).

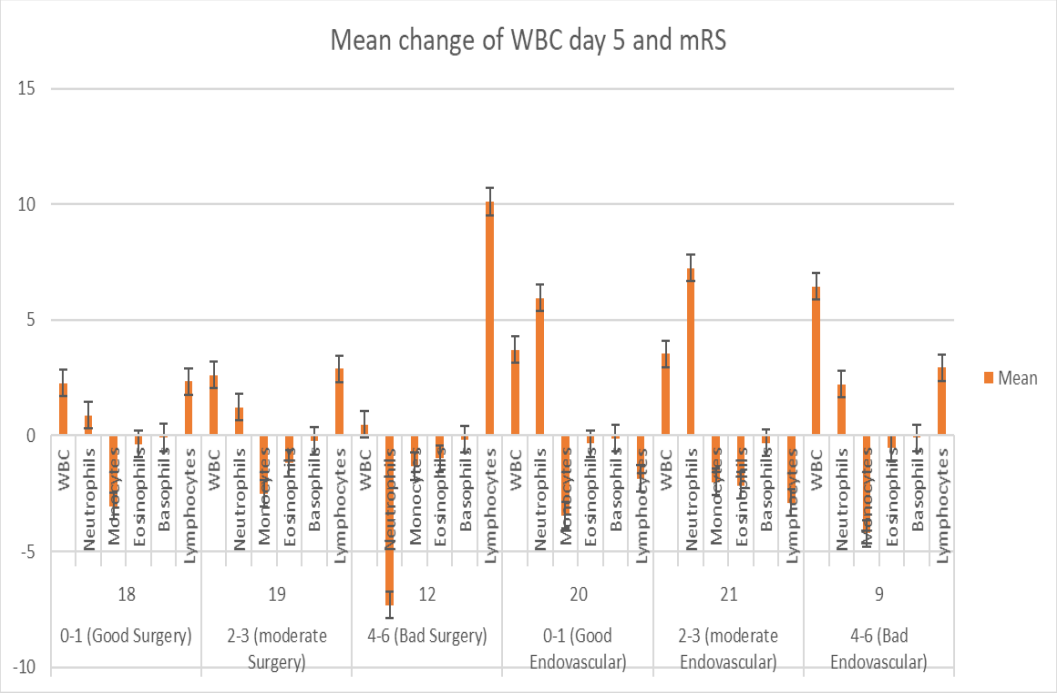


**Figure 11 mRS and WBC day 5 post-intervention**.

This chart shows the mean change of WBC on day 5 and the association with mRS categories in both surgery and endovascular groups. There is a negative association between neutrophil counts and mRS (*p = 0.07)*.

## Table 14 Change in WBC count from baseline day 5 and mRS

| sheet | mRS | N Obs | Variable | N | Mean change | Std Dev |
|---|---|---|---|---|---|---|
| 1 | 0–1 (Good) | 18 | d_day5_wbc | 18 | 2.26 | 2.75 |
| | | | d_day5_neutro | 18 | 0.88 | 12.27 |
| | | | d_day5_mono | 18 | -3.06 | 2.87 |
| | | | d_day5_esino | 18 | -0.36 | 1.69 |
| | | | d_day5_baso | 18 | -0.07 | 0.17 |
| | | | d_day5_lympho | 18 | 2.33 | 9.91 |
| | 2–3 (moderate) | 19 | d_day5_wbc | 19 | 2.62 | 4.86 |
| | | | d_day5_neutro | 18 | 1.22 | 19.22 |
| | | | d_day5_mono | 18 | -2.50 | 2.68 |
| | | | d_day5_esino | 18 | -1.18 | 2.18 |
| | | | d_day5_baso | 18 | -0.22 | 0.46 |
| | | | d_day5_lympho | 18 | 2.88 | 16.05 |
| | 4–6 (bad) | 12 | d_day5_wbc | 12 | 0.49 | 4.69 |
| | | | d_day5_neutro | 9 | -7.33 | 15.15 |
| | | | d_day5_mono | 9 | -1.32 | 3.78 |
| | | | d_day5_esino | 9 | -0.98 | 1.54 |
| | | | d_day5_baso | 9 | -0.15 | 0.27 |
| | | | d_day5_lympho | 9 | 10.11 | 13.86 |
| 2 | 0–1 (good) | 20 | d_day5_wbc | 20 | 3.71 | 3.22 |
| | | | d_day5_neutro | 20 | 5.95 | 12.74 |
| | | | d_day5_mono | 20 | -3.45 | 4.07 |
| | | | d_day5_esino | 20 | -0.33 | 1.71 |
| | | | d_day5_baso | 20 | -0.10 | 0.16 |
| | | | d_day5_lympho | 20 | -1.85 | 9.91 |
| | 2–3 (moderate) | 21 | d_day5_wbc | 20 | 3.54 | 5.17 |
| | | | d_day5_neutro | 20 | 7.25 | 9.89 |
| | | | d_day5_mono | 20 | -2.00 | 2.90 |
| | | | d_day5_esino | 20 | -2.16 | 5.15 |
| | | | d_day5_baso | 20 | -0.31 | 0.65 |
| | | | d_day5_lympho | 20 | -2.90 | 7.83 |
| | 4–6 (bad) | 9 | d_day5_wbc | 9 | 6.45 | 3.67 |
| | | | d_day5_neutro | 9 | 2.22 | 19.71 |
| | | | d_day5_mono | 9 | -4.22 | 2.72 |
| | | | d_day5_esino | 9 | -0.54 | 1.45 |
| | | | d_day5_baso | 9 | -0.08 | 0.17 |
| | | | d_day5_lympho | 9 | 2.94 | 17.6 |

Comparing maximum WBC counts changes after the procedures, neutrophils were decreased in number while lymphocytes were increased in both groups (Figure 12, Table 15). The association between these changes and mRS was not significant ($p > 0.05$).

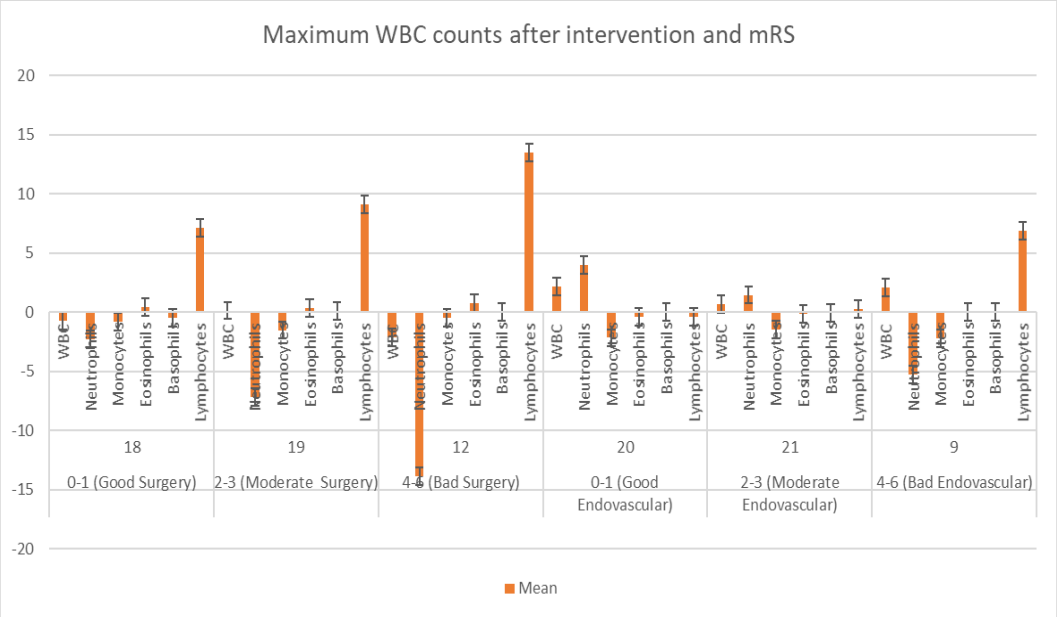


**Figure 12 Mean maximum change in WBC and mRS**.

Chart showing the interactions of mean WBC maximum counts and mRS post-surgery and endovascular groups. There is a lower number of neutrophils and more lymphocytes in the bad outcome groups (mRS 4-6; $p > 0,05$).

## Table 15 Change in maximum WBC count from baseline day 5 and mRS

| sheet | mRS | N Obs | Variable | N | Mean change | Std Dev |
|---|---|---|---|---|---|---|
| 1 | 0–1 (good) | 18 | d_max_wbc | 18 | -0.68 | 2.83 |
| | | | d_max_neutro | 18 | -2.27 | 25.96 |
| | | | d_max_mono | 18 | -0.77 | 3.76 |
| | | | d_max_esino | 18 | 0.44 | 1.44 |
| | | | d_max_baso | 18 | -0.43 | 2.14 |
| | | | d_max_lympho | 18 | 7.11 | 10.27 |
| | 2–3 (moderate) | 19 | d_max_wbc | 19 | 0.15 | 4.93 |
| | | | d_max_neutro | 19 | -7.15 | 18.57 |
| | | | d_max_mono | 18 | -1.50 | 3.20 |
| | | | d_max_esino | 19 | 0.34 | 1.32 |
| | | | d_max_baso | 19 | 0.08 | 0.29 |
| | | | d_max_lympho | 19 | 9.12 | 14.78 |
| | 4–6 (Bad) | 12 | d_max_wbc | 12 | -2.09 | 3.35 |
| | | | d_max_neutro | 12 | -13.83 | 15.60 |
| | | | d_max_mono | 12 | -0.49 | 4.14 |
| | | | d_max_esino | 12 | 0.78 | 1.21 |
| | | | d_max_baso | 12 | 0.03 | 0.16 |
| | | | d_max_lympho | 12 | 13.50 | 14.12 |
| 2 | 0–1 (good) | 20 | d_max_wbc | 20 | 2.17 | 2.75 |
| | | | d_max_neutro | 20 | 4.00 | 10.35 |
| | | | d_max_mono | 20 | -2.15 | 3.21 |
| | | | d_max_esino | 20 | -0.36 | 1.71 |
| | | | d_max_baso | 20 | 1.38 | 0.10 |
| | | | d_max_lympho | 20 | -0.40 | 8.74 |
| | 2–3 (moderate) | 21 | d_max_wbc | 21 | 0.68 | 5.06 |
| | | | d_max_neutro | 21 | 1.47 | 12.20 |
| | | | d_max_mono | 21 | -1.44 | 3.04 |
| | | | d_max_esino | 21 | -0.10 | 0.89 |
| | | | d_max_baso | 21 | -0.03 | 0.095 |
| | | | d_max_lympho | 21 | 0.28 | 8.84 |
| | 4–6 (bad) | 9 | d_max_wbc | 9 | 2.11 | 5.18 |
| | | | d_max_neutro | 9 | -5.22 | 18.43 |
| | | | d_max_mono | 9 | -2.22 | 2.58 |
| | | | d_max_esino | 9 | 0.06 | 0.71 |
| | | | d_max_baso | 9 | 0 | 0 |
| | | | d_max_lympho | 9 | 6.88 | 15.87 |

**Evaluation of leukocyte ratios in association with outcomes**

Functional outcome was assessed with the modified Rankin scale with a good neurological outcome defined as a score of 0–3. Logistic regression was used to measure the association between NLR, MLR, ELR, and PLR at admission, day 5 and day 10 with odds of the poor outcome. After adjustment for age, poor neurological grade at admission and the presence of intraventricular hemorrhage, the results are as follow: 1) at admission, there is no association between the parameters evaluated and outcome. Not even in NLR. 2) at day 5, higher NLR and MLR were associated with lower odds of poor outcome (OR 0.88 [0.78, 0.96] and 0.34 [0.11, 0.98] respectively) and 3) at day 10, there is no association between the parameters evaluated and outcome. It is worth noting that there was no difference in inflammatory parameters between treatment approaches.

# 7. Discussion and Conclusions

## 7.1 Discussion

The pathophysiology of SAH is complex and is closely related to the degree of elevation of ICP. The sudden increase of ICP caused by SAH is associated with up to 35% decrease in CBF. However, this does not fully explain patients' outcomes. In the animal model, the blood is injected slowly to avoid a sudden increase in ICP that would confound results. Other mechanisms such as ischemia and inflammation probably play some major role in modifying the natural history of the disease. Inflammation involves many aspects ranging from simple cellular reactions to complex molecular and genetic phenotypes. Neuro-inflammation is being studied intensively to understand how it is associated with worse outcomes in patients with SAH. The most commonly reported model is the cisternal injection model, followed by the endovascular puncture model. These models have possible effects on pro-inflammatory pathways, leukocyte activation, vessel wall, BBB, MMPs, neuronal cell death, microglial response, and demyelination, as well as neurodegeneration. The prechiasmatic injection model reproduces the effects produced by SAH as it causes a significant decrease in CBF with acceptable mortality and reproducible pathological lesions (Sabri et al., 2009). This model differs from other described models in the literature, such as cisterna magna or endovascular perforation models, in that it assumes a fixed amount of blood volume in the subarachnoid space, and mimics anterior circulation SAH. It also has an acceptable mortality rate at 7 days post-hemorrhage and is proven to cause neuronal cell death in experimental studies (Kooijman et al., 2014). This study reproduced the prechiasmatic model with some modifications. For example, the amount of blood injected was increased to increase the blood volume in the cistern.

In our animal model, SAH induced damage to neurons. Our staining for damaged neurons, Fluoro-Jade suggested neurological damage at days 5 and 7, which could

be attributed to apoptosis, supported by a higher TUNEL signal on day 7. The absence of MFG-E8 was associated with more damage as a trend for a higher number of degenerated neuronal cells was observed in that group. This could be attributed to increased microglial activation and decreased phagocytic ability, which can also induce more inflammation when neurons undergo secondary necrosis. It would be interesting to evaluate whether MFG-E8 administration would reduce apoptotic neurons, inflammation and improve neurological clinical scores. However, Fluoro-jade staining is technically difficult. Its use on frozen-fixed sections gave unsatisfactory background staining and multiple trials were needed to obtain an acceptable signal that was used for the analysis presented here. Furthermore, high intrinsic variability means larger sample sizes are needed to improve the ability to detect treatment effects (Schuller et al., 2013). The TUNEL staining was not highly specific and it was associated with strong background noise. However, both techniques were suggesting that our model was inducing neurological damage as found in SAH patients. We recently established the model in the laboratory. The trends that were observed here, were confirmed in subsequent work from the group. Phenotypic assessment of SAH mice would also represent an additional tool to demonstrate the efficacy of the model. Other methods such as caspase-3 staining, could be used to demonstrate that our model induced more neuronal apoptosis. Despite the findings for neuronal damage by apoptosis after SAH, there is no consensus that neuronal apoptotic cell death occurs after SAH and other mechanisms (e.g., necrosis, autophagy, or reduction of neuron numbers due to their phagocytosis) may be at work.

Our results suggested an increased intracerebral presence of macrophages/microglia on day 5 and 7, as well as more neutrophils in the brains of SAH animals. Similarly, increased microglial activation was observed in later work from the laboratory. This suggests that SAH induced intracerebral inflammation enhancing monocyte recruitment. We only looked at numbers, however, phenotypic evaluation of microglial activation could be measured. It is possible to test for microglia and astrocytes activation using Iba-1 (Ionized Calcium-binding adaptor molecule-1) and GFAP (Glial Fibrillary Acidic Protein)

cell markers respectively. Unfortunately, many of our observations did not reach clinical significance and a larger number of animals might be needed to see the difference. As stated previously, our results were confirmed. The H and E slides showed no infiltrates or gross necrosis. Further experiments in the laboratory confirmed these observations, highlighting the presence of damaged and dead neurons to confirm that the model can reproduce the functional deficit found in SAH patients (Al-Khindi et al., 2010). Moreover, there are currently no widely accepted specific markers for each cell type to allow testing microglia/ macrophages separately. Isolation of brain infiltrating leukocyte would help to determine their respective phenotype identifying cells with low CD11b+/CD45 as microglia and cells with high CD11b+/CD45 as macrophages (Denker et al., 2007). Ongoing experiments in our laboratory use Iba-1 staining to identify activated microglia, with promising results, but it can also react with macrophages. Therefore, future work could use these methods (Bennett et al., 2016). We used F4/80 to evaluate the level of brain phagocyte infiltration into the CNS because this antibody is specific for macrophages. MPO staining results might suggest that there are more neutrophils in the SAH group. However, the staining was not highly specific and the number of mice was too small to conclude; further experiments are needed to confirm our observations.

It should be noted that the presented experimental work was at the preliminary stage. Since my presence in the laboratory, the number of animals used has been increased to have statistical power and to prove the presence of inflammation and neuronal cell death.

There is evidence that systemic inflammatory response syndrome occurs early after SAH (Zhong et al., 2017), manifested by increased peripheral WBC counts, fever, and high heart and respiratory rates. With our retrospective study, we wanted to highlight any modulation in the inflammatory reaction induced by SAH by looking at leukocyte counts. We observed an initial leukocytosis evident in patients with SAH, which reached its maximum at approximately 2 days after any procedure. The maximum leukocytosis was higher in the surgical group ($p$ = 0.029), reflecting the additional inflammatory effect of surgery relative to the

endovascular group. Whether this leukocytosis is due to increased production, demargination or other mechanisms is to be determined by more detailed studies. This could mean that minimally invasive or brain-no-touch technique could decrease the degree of inflammation already present due to the SAH (Agrawal et al., 2016). However, these observations need to be confirmed with a larger number of patients. The analysis also showed that leukocytosis returns to normal in both groups at approximately 5 days, which could indicate the end of bone marrow mobilization. The observed higher maximum lymphocyte counts in the endovascular group could point towards a direct effect of the endovascular manipulation on peripheral immune cells recruitment, which needs further attention in the future. There was essentially no difference in outcomes between surgical and endovascular groups when looking in the interaction between leukocytosis, leukocyte subsets, and mRS score. However, we found that a higher NLR and MLR were associated with lower odds of poor outcome (OR 0.88 [0.78, 0.96] and 0.34 [0.11, 0.98] respectively). This suggests that neutrophils and monocytes may have a positive impact on reducing DCI. However, this is still very exploratory to conclude. This could be explained by the fact that both cell types can adopt anti-inflammatory phenotype (Durafourt et al., 2012a, Leidi et al., 2009). However, inflammation is induced by aging, diseases such as hypertension, chronic renal failure, diabetes, dyslipidemia, all that can be found in the SAH patient population (Lecube et al., 2011, Frostegard, 2013, Shaw et al., 2013). Thus, it may be difficult to highlight a specific immunological signature induced by SAH above the occurring inflammatory background present in these patients.

The clinical analysis is limited by the fact that it is retrospective and only focused on peripheral leukocyte counts. Another study limitation is that measuring the inflammatory effect on delayed outcomes needs a larger patient number and more prospective protocols to decrease the effect of confounders. The laboratory is undergoing prospective immune monitoring of SAH patients to decipher immune activation in this patient population. This will be highly relevant to evaluate the respective roles of each leukocyte subsets.

## 7.2 Conclusion and Perspectives

The aim of understanding inflammation in SAH is to find ways to save neurons and limit the neuronal damage, which is the only way to save brain function. This study validated the animal model by the presence of blood. We would also need to control all aspects of the pathophysiology, such as ICP monitoring and measuring blood flow. Neuronal damage was evident in SAH mice at days 5 and 7 and might have been due to inflammation manifested by increased microglia and macrophage number. This inflammation may be responsible for the patient's poor long-term prognoses. The nature of the inflammation in our model has been confirmed since, which reproduced what is seen in patients. Therefore, this model could be considered as clinically relevant and used to test treatments that may have more chance of successfully helping SAH patients. Our laboratory is working on modulators of inflammation such as MFG-E8 and its role in reducing inflammation and neurological damage in our animal SAH model. This would represent a novel treatment for this patient population in need. Measuring inflammation in clinical practice is often challenging and specific inflammatory markers for SAH do not exist. We showed that leukocytosis is present in most SAH patients and that ratios of neutrophils and monocytes to lymphocytes are associated with a better outcome, suggesting that phenotyping evaluation of leukocyte phenotype is warranted. Reproducing and confirming our preliminary results using large patient databases and identifying better parameters to measure brain inflammation in SAH are needed to better understand the relationship between inflammation and patient outcomes. However, SAH studies to date have lacked an integrated understanding of the activation of the immune system. Deciphering the immunological signature of SAH by evaluating comprehensively the immune cell phenotypes and cytokines will identify new mediators that could be modulated to help this patient population in need of new treatment modalities.

# Bibliography


AGRAWAL, D., KURWALE, N. & SHARMA, B. S. 2016. Leukocytosis after routine cranial surgery: A potential marker for brain damage in intracranial surgery. *Asian J Neurosurg,* 11**,** 109-13.

AL-KHINDI, T., MACDONALD, R. L. & SCHWEIZER, T. A. 2010. Cognitive and functional outcome after aneurysmal subarachnoid hemorrhage. *Stroke,* 41**,** e519-36.

ARSLAN, F., KEOGH, B., MCGUIRK, P. & PARKER, A. E. 2010. TLR2 and TLR4 in ischemia reperfusion injury. *Mediators Inflamm,* 2010**,** 704202.

BABCOCK, A. A., WIRENFELDT, M., HOLM, T., NIELSEN, H. H., DISSING-OLESEN, L., TOFT-HANSEN, H., MILLWARD, J. M., LANDMANN, R., RIVEST, S., FINSEN, B. & OWENS, T. 2006. Toll-like receptor 2 signaling in response to brain injury: an innate bridge to neuroinflammation. *J Neurosci,* 26**,** 12826-37.

BARONE, F. C., HILLEGASS, L. M., PRICE, W. J., WHITE, R. F., LEE, E. V., FEUERSTEIN, G. Z., SARAU, H. M., CLARK, R. K. & GRISWOLD, D. E. 1991. Polymorphonuclear leukocyte infiltration into cerebral focal ischemic tissue: myeloperoxidase activity assay and histologic verification. *J Neurosci Res,* 29**,** 336-45.

BARONE, F. C., LYSKO, P. G., PRICE, W. J., FEUERSTEIN, G., AL-BARACANJI, K. A., BENHAM, C. D., HARRISON, D. C., HARRIES, M. H., BAILEY, S. J. & HUNTER, A. J. 1995. SB 201823-A Antagonizes Calcium Currents in Central Neurons and Reduces the Effects of Focal Ischemia in Rats and Mice. *Stroke,* 26**,** 1683-1690.

BARROS, M. H., HAUCK, F., DREYER, J. H., KEMPKES, B. & NIEDOBITEK, G. 2013. Macrophage polarisation: an immunohistochemical approach for identifying M1 and M2 macrophages. *PLoS One,* 8**,** e80908.

BECHMANN, I., GOLDMANN, J., KOVAC, A. D., KWIDZINSKI, E., SIMBURGER, E., NAFTOLIN, F., DIRNAGL, U., NITSCH, R. & PRILLER, J. 2005. Circulating monocytic cells infiltrate layers of anterograde axonal degeneration where they transform into microglia. *FASEB J,* 19**,** 647-9.

BENNETT, M. L., BENNETT, F. C., LIDDELOW, S. A., AJAMI, B., ZAMANIAN, J. L., FERNHOFF, N. B., MULINYAWE, S. B., BOHLEN, C. J., ADIL, A., TUCKER, A., WEISSMAN, I. L., CHANG, E. F., LI, G., GRANT, G. A., HAYDEN GEPHART, M. G. & BARRES, B. A. 2016. New tools for studying microglia in the mouse and human CNS. *Proc Natl Acad Sci U S A,* 113**,** E1738-46.

BILLINGHAM, R. E. & BOSWELL, T. 1953. Studies on the problem of corneal homografts. *Proc R Soc Lond B Biol Sci,* 141**,** 392-406.

BRISSETTE, M. J., LAPLANTE, P., QI, S., LATOUR, M. & CAILHIER, J. F. 2016. Milk fat globule epidermal growth factor-8 limits tissue damage through inflammasome modulation during renal injury. *J Leukoc Biol,* 100**,** 1135-1146.

BUCK, B. H., LIEBESKIND, D. S., SAVER, J. L., BANG, O. Y., YUN, S. W., STARKMAN, S., ALI, L. K., KIM, D., VILLABLANCA, J. P., SALAMON, N., RAZINIA, T. & OVBIAGELE, B. 2008. Early neutrophilia is associated with volume of ischemic tissue in acute stroke. *Stroke,* 39**,** 355-60.

CHAPMAN, K. Z., DALE, V. Q., DENES, A., BENNETT, G., ROTHWELL, N. J., ALLAN, S. M. & MCCOLL, B. W. 2009. A rapid and transient peripheral inflammatory response precedes brain inflammation after experimental stroke. *J Cereb Blood Flow Metab,* 29**,** 1764-8.

CHOI, S. H., VEERARAGHAVALU, K., LAZAROV, O., MARLER, S., RANSOHOFF, R. M., RAMIREZ, J. M. & SISODIA, S. S. 2008. Non-cell-autonomous effects of presenilin 1 variants on enrichment-mediated hippocampal progenitor cell proliferation and differentiation. *Neuron,* 59**,** 568-80.

CONNOLLY, E. S., JR., RABINSTEIN, A. A., CARHUAPOMA, J. R., DERDEYN, C. P., DION, J., HIGASHIDA, R. T., HOH, B. L., KIRKNESS, C. J., NAIDECH, A. M., OGILVY, C. S., PATEL, A. B., THOMPSON, B. G., VESPA, P., AMERICAN HEART ASSOCIATION STROKE, C., COUNCIL ON CARDIOVASCULAR, R., INTERVENTION, COUNCIL ON CARDIOVASCULAR, N., COUNCIL ON CARDIOVASCULAR, S., ANESTHESIA & COUNCIL ON CLINICAL, C. 2012. Guidelines for the management of aneurysmal subarachnoid hemorrhage: a guideline for healthcare professionals from the American Heart Association/american Stroke Association. *Stroke,* 43**,** 1711-37.

D'SOUZA, S. 2015. Aneurysmal Subarachnoid Hemorrhage. *J Neurosurg Anesthesiol,* 27**,** 222-40.

DA SILVA, I. R. F., GOMES, J. A., WACHSMAN, A., DE FREITAS, G. R. & PROVENCIO, J. J. 2017. Hematologic counts as predictors of delayed cerebral ischemia after aneurysmal subarachnoid hemorrhage. *J Crit Care,* 37**,** 126-129.

DE OLIVEIRA MANOEL, A. L. & MACDONALD, R. L. 2018. Neuroinflammation as a Target for Intervention in Subarachnoid Hemorrhage. *Front Neurol,* 9**,** 292.

DENKER, S. P., JI, S., DINGMAN, A., LEE, S. Y., DERUGIN, N., WENDLAND, M. F. & VEXLER, Z. S. 2007. Macrophages are comprised of resident brain microglia not infiltrating peripheral monocytes acutely after neonatal stroke. *J Neurochem,* 100**,** 893-904.

DHAR, R. & DIRINGER, M. N. 2008. The burden of the systemic inflammatory response predicts vasospasm and outcome after subarachnoid hemorrhage. *Neurocrit Care,* 8**,** 404-12.

DIETEL, B., CICHA, I., KALLMUNZER, B., TAUCHI, M., YILMAZ, A., DANIEL, W. G., SCHWAB, S., GARLICHS, C. D. & KOLLMAR, R. 2012. Suppression of dendritic cell functions contributes to the anti-inflammatory action of granulocyte-colony stimulating factor in experimental stroke. *Exp Neurol,* 237**,** 379-87.

DIRNAGL, U., IADECOLA, C. & MOSKOWITZ, M. A. 1999. Pathobiology of ischaemic stroke: an integrated view. *Trends in Neurosciences,* 22**,** 391-397.

DURAFOURT, B., MOORE, C., BAR-OR, A. & ANTEL, J. 2012a. Relation of Myelin Ingestion with Distinct Polarization Properties of Human Adult Microglia Versus Blood-Derived Macrophages (P02.102). *Neurology,* 78**,** P02.102-P02.102.

DURAFOURT, B. A., MOORE, C. S., ZAMMIT, D. A., JOHNSON, T. A., ZAGUIA, F., GUIOT, M. C., BAR-OR, A. & ANTEL, J. P. 2012b. Comparison of polarization properties of human adult microglia and blood-derived macrophages. *Glia,* 60**,** 717-27.

DYRNA, F., HANSKE, S., KRUEGER, M. & BECHMANN, I. 2013. The blood-brain barrier. *J Neuroimmune Pharmacol,* 8**,** 763-73.

FANG, R., ZHENG, X. & ZHANG, M. 2016. Ethyl pyruvate alleviates early brain injury following subarachnoid hemorrhage in rats. *Acta Neurochir (Wien),* 158**,** 1069-76.

FROSEN, J., TULAMO, R., PAETAU, A., LAAKSAMO, E., KORJA, M., LAAKSO, A., NIEMELA, M. & HERNESNIEMI, J. 2012. Saccular intracranial aneurysm: pathology and mechanisms. *Acta Neuropathol,* 123**,** 773-86.

FROSTEGARD, J. 2013. Immunity, atherosclerosis and cardiovascular disease. *BMC Med,* 11**,** 117.

HANISCH, U. K. & KETTENMANN, H. 2007. Microglia: active sensor and versatile effector cells in the normal and pathologic brain. *Nat Neurosci,* 10**,** 1387-94.

HANKE, M. L. & KIELIAN, T. 2011. Toll-like receptors in health and disease in the brain: mechanisms and therapeutic potential. *Clin Sci (Lond),* 121**,** 367-87.

HU, X., LI, P., GUO, Y., WANG, H., LEAK, R. K., CHEN, S., GAO, Y. & CHEN, J. 2012. Microglia/macrophage polarization dynamics reveal novel mechanism of injury expansion after focal cerebral ischemia. *Stroke,* 43**,** 3063-70.

IADECOLA, C. 2004. Neurovascular regulation in the normal brain and in Alzheimer's disease. *Nat Rev Neurosci,* 5**,** 347-60.

IWATA, A., MORGAN-STEVENSON, V., SCHWARTZ, B., LIU, L., TUPPER, J., ZHU, X., HARLAN, J. & WINN, R. 2010. Extracellular BCL2 proteins are danger-associated molecular patterns that reduce tissue damage in murine models of ischemia-reperfusion injury. *PLoS One,* 5**,** e9103.

JACK, C. S., ARBOUR, N., MANUSOW, J., MONTGRAIN, V., BLAIN, M., MCCREA, E., SHAPIRO, A. & ANTEL, J. P. 2005. TLR Signaling Tailors Innate Immune Responses in Human Microglia and Astrocytes. *The Journal of Immunology,* 175**,** 4320-4330.

JELENA, P.-V., DUNJA, G., ARSEN, U., MARIJA, G., GORDANA, J. & VLADIMIR, V. 2015. Prognostic Significance of Hyponatremia Leukocytosis, Hypomagnesemia, and Fever after Aneurysmal Subarachnoid Hemorrhage. *Indian Journal of Neurosurgery,* 04**,** 069-073.

KADIRVEL, R., DING, Y. H., DAI, D., ZAKARIA, H., ROBERTSON, A. M., DANIELSON, M. A., LEWIS, D. A., CLOFT, H. J. & KALLMES, D. F. 2007. The influence of hemodynamic forces on biomarkers in the walls of elastase-induced aneurysms in rabbits. *Neuroradiology,* 49**,** 1041-53.

KAWABORI, M. & YENARI, M. A. 2015. The role of the microglia in acute CNS injury. *Metab Brain Dis,* 30**,** 381-92.

KIERDORF, K. & PRINZ, M. 2013. Factors regulating microglia activation. *Front Cell Neurosci,* 7**,** 44.

KITAMURA, T. 1973. The Origin of Brain Macrophages - Some Considerations on the Microglia Theory of Del Rio-Hortega. *Pathology International,* 23**,** 11-26.

KOOIJMAN, E., NIJBOER, C. H., VAN VELTHOVEN, C. T., KAVELAARS, A., KESECIOGLU, J. & HEIJNEN, C. J. 2014. The rodent endovascular puncture model of subarachnoid hemorrhage: mechanisms of brain damage and therapeutic strategies. *J Neuroinflammation,* 11**,** 2.

LAHIRI, S., KAMEL, H., MEYERS, E. E., FALO, M. C., AL-MUFTI, F., SCHMIDT, J. M., AGARWAL, S., PARK, S., CLAASSEN, J. & MAYER, S. A. 2016. Patient-Powered Reporting of Modified Rankin Scale Outcomes Via the Internet. *Neurohospitalist,* 6**,** 11-3.

LANTIGUA, H., ORTEGA-GUTIERREZ, S., SCHMIDT, J. M., LEE, K., BADJATIA, N., AGARWAL, S., CLAASSEN, J., CONNOLLY, E. S. & MAYER, S. A. 2015. Subarachnoid hemorrhage: who dies, and why? *Crit Care,* 19**,** 309.

LAPLANTE, P., BRILLANT-MARQUIS, F., BRISSETTE, M. J., JOANNETTE-PILON, B., CAYROL, R., KOKTA, V. & CAILHIER, J. F. 2017. MFG-E8 Reprogramming of Macrophages Promotes Wound Healing by Increased bFGF Production and Fibroblast Functions. *J Invest Dermatol,* 137**,** 2005-2013.

LARYSZ-BRYSZ, M., LEWIN-KOWALIK, J., CZUBA, Z., KOTULSKA, K., OLAKOWSKA, E., MARCOL, W., LISKIEWICZ, A. & JEDRZEJOWSKA-SZYPULKA, H. 2012. Interleukin-1&bgr; Increases Release of Endothelin-1 and Tumor Necrosis Factor as Well as Reactive Oxygen Species by Peripheral Leukocytes During Experimental Subarachnoid Hemorrhage. *Current Neurovascular Research,* 9**,** 159-166.

LECUBE, A., PACHON, G., PETRIZ, J., HERNANDEZ, C. & SIMO, R. 2011. Phagocytic activity is impaired in type 2 diabetes mellitus and increases after metabolic improvement. *PLoS One,* 6**,** e23366.

LEE, H., PERRY, J. J., ENGLISH, S. W., ALKHERAYF, F., JOSEPH, J., NOBILE, S., ZHOU, L. L., LESIUK, H., MOULTON, R., AGBI, C., SINCLAIR, J. & DOWLATSHAHI, D. 2018. Clinical prediction of delayed cerebral ischemia in aneurysmal subarachnoid hemorrhage. *J Neurosurg***,** 1-8.

LEIDI, M., GOTTI, E., BOLOGNA, L., MIRANDA, E., RIMOLDI, M., SICA, A., RONCALLI, M., PALUMBO, G. A., INTRONA, M. & GOLAY, J. 2009. M2 macrophages phagocytose rituximab-opsonized leukemic targets more efficiently than m1 cells in vitro. *J Immunol,* 182**,** 4415-22.

LIU, F., HU, Q., LI, B., MANAENKO, A., CHEN, Y., TANG, J., GUO, Z., TANG, J. & ZHANG, J. H. 2014. Recombinant milk fat globule-EGF factor-8 reduces oxidative stress via integrin beta3/nuclear factor erythroid 2-related factor 2/heme oxygenase pathway in subarachnoid hemorrhage rats. *Stroke,* 45**,** 3691-7.

LO, B. W., FUKUDA, H., NISHIMURA, Y., FARROKHYAR, F., THABANE, L. & LEVINE, M. A. 2015. Systematic review of clinical prediction tools and prognostic factors in aneurysmal subarachnoid hemorrhage. *Surg Neurol Int,* 6**,** 135.

LOUVEAU, A., SMIRNOV, I., KEYES, T. J., ECCLES, J. D., ROUHANI, S. J., PESKE, J. D., DERECKI, N. C., CASTLE, D., MANDELL, J. W., LEE, K. S., HARRIS, T. H. & KIPNIS, J. 2015. Structural and functional features of central nervous system lymphatic vessels. *Nature,* 523**,** 337-41.

LUCKE-WOLD, B. P., LOGSDON, A. F., MANORANJAN, B., TURNER, R. C., MCCONNELL, E., VATES, G. E., HUBER, J. D., ROSEN, C. L. & SIMARD, J. M. 2016. Aneurysmal Subarachnoid Hemorrhage and Neuroinflammation: A Comprehensive Review. *Int J Mol Sci,* 17**,** 497.

LUO, C., YAO, X., LI, J., HE, B., LIU, Q., REN, H., LIANG, F., LI, M., LIN, H., PENG, J., YUAN, T. F., PEI, Z. & SU, H. 2016. Paravascular pathways contribute to vasculitis and neuroinflammation after subarachnoid hemorrhage independently of glymphatic control. *Cell Death Dis,* 7**,** e2160.

MACDONALD, R. L. 2014. Delayed neurological deterioration after subarachnoid haemorrhage. *Nat Rev Neurol,* 10**,** 44-58.

MARS, L. T., SAIKALI, P., LIBLAU, R. S. & ARBOUR, N. 2011. Contribution of CD8 T lymphocytes to the immuno-pathogenesis of multiple sclerosis and its animal models. *Biochim Biophys Acta,* 1812**,** 151-61.

MCBRIDE, D. W., BLACKBURN, S. L., PEEYUSH, K. T., MATSUMURA, K. & ZHANG, J. H. 2017. The Role of Thromboinflammation in Delayed Cerebral Ischemia after Subarachnoid Hemorrhage. *Front Neurol,* 8**,** 555.

MCFARLAND, H. F. & MARTIN, R. 2007. Multiple sclerosis: a complicated picture of autoimmunity. *Nat Immunol,* 8**,** 913-9.

MCGIRT, M. J., MAVROPOULOS, J. C., MCGIRT, L. Y., ALEXANDER, M. J., FRIEDMAN, A. H., LASKOWITZ, D. T. & LYNCH, J. R. 2003. Leukocytosis as an independent risk factor for cerebral vasospasm following aneurysmal subarachnoid hemorrhage. *J Neurosurg,* 98**,** 1222-6.

MEDAWAR, P. B. 1948. Immunity to Homologous Grafted Skin. III. The Fate of Skin Homographs Transplanted to the Brain, to Subcutaneous Tissue, and to the Anterior Chamber of the Eye. *Br J Exp Pathol.,* 29(1)**,** 58–69.

MEDIC, N., LORENZON, P., VITA, F., TREVISAN, E., MARCHIOLI, A., SORANZO, M. R., FABBRETTI, E. & ZABUCCHI, G. 2010. Mast cell adhesion induces cytoskeletal modifications and programmed cell death in oligodendrocytes. *J Neuroimmunol,* 218**,** 57-66.

MENG, H., TUTINO, V. M., XIANG, J. & SIDDIQUI, A. 2014. High WSS or low WSS? Complex interactions of hemodynamics with intracranial aneurysm initiation, growth, and rupture: toward a unifying hypothesis. *AJNR Am J Neuroradiol,* 35**,** 1254-62.

MENG, H., WANG, Z., HOI, Y., GAO, L., METAXA, E., SWARTZ, D. D. & KOLEGA, J. 2007. Complex hemodynamics at the apex of an arterial bifurcation induces vascular remodeling resembling cerebral aneurysm initiation. *Stroke,* 38**,** 1924-31.

MILDNER, A., SCHMIDT, H., NITSCHE, M., MERKLER, D., HANISCH, U. K., MACK, M., HEIKENWALDER, M., BRUCK, W., PRILLER, J. & PRINZ, M. 2007. Microglia in the adult brain arise from Ly-6ChiCCR2+ monocytes only under defined host conditions. *Nat Neurosci,* 10**,** 1544-53.

MILLER, B. A., TURAN, N., CHAU, M. & PRADILLA, G. 2014. Inflammation, vasospasm, and brain injury after subarachnoid hemorrhage. *Biomed Res Int,* 2014**,** 384342.

MILLER, S. D., MCMAHON, E. J., SCHREINER, B. & BAILEY, S. L. 2007. Antigen presentation in the CNS by myeloid dendritic cells drives progression of relapsing experimental autoimmune encephalomyelitis. *Ann N Y Acad Sci,* 1103**,** 179-91.

MORAES, L., GRILLE, S., MORELLI, P., MILA, R., TRIAS, N., BRUGNINI, A., N, L. L., BIESTRO, A. & LENS, D. 2015. Immune cells subpopulations in cerebrospinal fluid and peripheral blood of patients with Aneurysmal Subarachnoid Hemorrhage. *Springerplus,* 4**,** 195.

MRACSKO, E. & VELTKAMP, R. 2014. Neuroinflammation after intracerebral hemorrhage. *Front Cell Neurosci,* 8**,** 388.

MULDOON, L. L., ALVAREZ, J. I., BEGLEY, D. J., BOADO, R. J., DEL ZOPPO, G. J., DOOLITTLE, N. D., ENGELHARDT, B., HALLENBECK, J. M., LONSER, R. R., OHLFEST, J. R., PRAT, A., SCARPA, M., SMEYNE, R. J., DREWES, L. R. & NEUWELT, E. A. 2013. Immunologic privilege in the central nervous system and the blood-brain barrier. *J Cereb Blood Flow Metab,* 33**,** 13-21.

NEHER, J. J., EMMRICH, J. V., FRICKER, M., MANDER, P. K., THERY, C. & BROWN, G. C. 2013. Phagocytosis executes delayed neuronal death after focal brain ischemia. *Proc Natl Acad Sci U S A,* 110**,** E4098-107.

OLIVEIRA-FILHO, J., EZZEDDINE, M. A., SEGAL, A. Z., BUONANNO, F. S., CHANG, Y., OGILVY, C. S., RORDORF, G., SCHWAMM, L. H., KOROSHETZ, W. J. & MCDONALD, C. T. 2001. Fever in subarachnoid hemorrhage: Relationship to vasospasm and outcome. *Neurology,* 56**,** 1299-1304.

PIERSON, E. R., WAGNER, C. A. & GOVERMAN, J. M. 2018. The contribution of neutrophils to CNS autoimmunity. *Clin Immunol,* 189**,** 23-28.

PRINZ, M., PRILLER, J., SISODIA, S. S. & RANSOHOFF, R. M. 2011. Heterogeneity of CNS myeloid cells and their roles in neurodegeneration. *Nat Neurosci,* 14**,** 1227-35.

PRODINGER, C., BUNSE, J., KRUGER, M., SCHIEFENHOVEL, F., BRANDT, C., LAMAN, J. D., GRETER, M., IMMIG, K., HEPPNER, F., BECHER, B. & BECHMANN, I. 2011. CD11c-expressing cells reside in the juxtavascular parenchyma and extend processes into the glia limitans of the mouse nervous system. *Acta Neuropathol,* 121**,** 445-58.

PROVENCIO, J. J., SWANK, V., LU, H., BRUNET, S., BALTAN, S., KHAPRE, R. V., SEERAPU, H., KOKIKO-COCHRAN, O. N., LAMB, B. T. & RANSOHOFF, R. M. 2016. Neutrophil depletion after subarachnoid hemorrhage improves memory via NMDA receptors. *Brain Behav Immun,* 54**,** 233-242.

RABINSTEIN, A. A. 2011. Secondary brain injury after aneurysmal subarachnoid haemorrhage: more than vasospasm. *The Lancet Neurology,* 10**,** 593-595.

RINKEL, G. J. E. & ALGRA, A. 2011. Long-term outcomes of patients with aneurysmal subarachnoid haemorrhage. *The Lancet Neurology,* 10**,** 349-356.

RIVERO RODRIGUEZ, D., SCHERLE MATAMOROS, C., CUE, L. F., MIRANDA HERNANDEZ, J. L., PERNAS SANCHEZ, Y. & PEREZ NELLAR, J. 2015. Predictor's of Mortality in Patients with Aneurysmal Subarachnoid Haemorrhage and Reebleding. *Neurol Res Int,* 2015**,** 545407.

ROCK, R. B., GEKKER, G., HU, S., SHENG, W. S., CHEERAN, M., LOKENSGARD, J. R. & PETERSON, P. K. 2004. Role of microglia in central nervous system infections. *Clin Microbiol Rev,* 17**,** 942-64

ROSEN, D. S. & MACDONALD, R. L. 2005. Subarachnoid Hemorrhage Grading Scales: A Systematic Review. *Neurocritical Care,* 2**,** 110-118.

RUIGROK, Y. M. & RINKEL, G. J. 2008. Genetics of intracranial aneurysms. *Stroke,* 39**,** 1049-55.

SABRI, M., JEON, H., AI, J., TARIQ, A., SHANG, X., CHEN, G. & MACDONALD, R. L. 2009. Anterior circulation mouse model of subarachnoid hemorrhage. *Brain Res,* 1295**,** 179-85.

SCHAFER, D. P., LEHRMAN, E. K., KAUTZMAN, A. G., KOYAMA, R., MARDINLY, A. R., YAMASAKI, R., RANSOHOFF, R. M., GREENBERG, M. E., BARRES, B. A. & STEVENS, B. 2012. Microglia sculpt postnatal neural circuits in an activity and complement-dependent manner. *Neuron,* 74**,** 691-705.

SCHAFER, D. P., LEHRMAN, E. K. & STEVENS, B. 2013. The "quad-partite" synapse: microglia-synapse interactions in the developing and mature CNS. *Glia,* 61**,** 24-36.

SCHNEIDER, U. C., DAVIDS, A.-M., BRANDENBURG, S., MÜLLER, A., ELKE, A., MAGRINI, S., ATANGANA, E., TURKOWSKI, K., FINGER, T., GUTENBERG, A.,

GEHLHAAR, C., BRÜCK, W., HEPPNER, F. L. & VAJKOCZY, P. 2015. Microglia inflict delayed brain injury after subarachnoid hemorrhage. *Acta Neuropathologica,* 130**,** 215-231.

SCHULLER, K., BUHLER, D. & PLESNILA, N. 2013. A murine model of subarachnoid hemorrhage. *J Vis Exp***,** e50845.

SEHBA, F. A. & BEDERSON, J. B. 2013. Mechanisms of acute brain injury after subarachnoid hemorrhage. *Neurological Research,* 28**,** 381-398.

SEHBA, F. A., MOSTAFA, G., KNOPMAN, J., FRIEDRICH, V., JR. & BEDERSON, J. B. 2004. Acute alterations in microvascular basal lamina after subarachnoid hemorrhage. *J Neurosurg,* 101**,** 633-40.

SHAW, A. C., GOLDSTEIN, D. R. & MONTGOMERY, R. R. 2013. Age-dependent dysregulation of innate immunity. *Nat Rev Immunol,* 13**,** 875-87.

SIEVERS, J., SCHMIDTMAYER, J. & PARWARESCH, R. 1994. Blood monocytes and spleen macrophages differentiate into microglia-like cells when cultured on astrocytes. *Annals of Anatomy - Anatomischer Anzeiger,* 176**,** 45-51.

SUN, B. L., XIE, F. M., YANG, M. F., CAO, M. Z., YUAN, H., WANG, H. T., WANG, J. R. & JIA, L. 2011. Blocking cerebral lymphatic drainage deteriorates cerebral oxidative injury in rats with subarachnoid hemorrhage. *Acta Neurochir Suppl,* 110**,** 49-53.

TIAN, L., MA, L., KAARELA, T. & LI, Z. 2012. Neuroimmune crosstalk in the central nervous system and its significance for neurological diseases. *J Neuroinflammation,* 9**,** 155.

VAN GIJN, J. & RINKEL, G. J. E. 2001. Subarachnoid haemorrhage: diagnosis, causes and management. *Brain,* 124**,** 249-278.

WALTON, J. N. 1952. Late Prognosis of Subarachnoid Haemorrhage. *Bmj,* 2**,** 802-808.

WOLF, S. 2013. Take care when taking care of fever after aneurysmal subarachnoid hemorrhage. *Crit Care,* 17**,** 160.

WONG, G. K. C. & POON, W. S. 2011. Clazosentan for patients with subarachnoid haemorrhage: lessons learned. *The Lancet Neurology,* 10.

YUKSEL, S., TOSUN, Y. B., CAHILL, J. & SOLAROGLU, I. 2012. Early brain injury following aneurysmal subarachnoid hemorrhage: emphasis on cellular apoptosis. *Turk Neurosurg,* 22**,** 529-33.

ZHANG, D., ZHANG, H., HAO, S., YAN, H., ZHANG, Z., HU, Y., ZHUANG, Z., LI, W., ZHOU, M., LI, K. & HANG, C. 2016. Akt Specific Activator SC79 Protects against Early Brain Injury following Subarachnoid Hemorrhage. *ACS Chem Neurosci,* 7**,** 710-8.

ZHONG, W., ZHANG, Z., ZHAO, P., SHEN, J., LI, X., WANG, D., LI, G. & SU, W. 2017. The Impact of Initial Systemic Inflammatory Response After Aneurysmal Subarachnoid Hemorrhage. *Turk Neurosurg,* 27**,** 346-352.

ZIELINSKI, C. E., MELE, F., ASCHENBRENNER, D., JARROSSAY, D., RONCHI, F., GATTORNO, M., MONTICELLI, S., LANZAVECCHIA, A. & SALLUSTO, F. 2012. Pathogen-induced human TH17 cells produce IFN-gamma or IL-10 and are regulated by IL-1beta. *Nature,* 484**,** 514-8.